Master thesis in physical oceanography

Argo Profiling Floats in the Nordic Seas: Deep-water circulation, hydrography and comparisons to the TOPAZ model

Katrine Dale Bjordal
May, 2006

Geophysical Institute
University of Bergen
Norway

Mohn-Sverdrup Center for
Global Ocean Studies and Operational Oceanography
Bergen, Norway

Acknowledgements

I would like to thank my supervisors Tor Gammelsrød and Johnny Johannessen for your support and guidance. Thanks for always keeping your office door open and for providing me with advice and help whenever needed. I would also like to thank my external supervisor, Laurent Bertino, for help and answers to (almost) all my questions! Thanks also to my external supervisor, Kjell Arne Mork for your guidance and your matlab advice.
Thanks to the Nansen Center and especially the Mohn-Sverdrup group for the friendly working environment. The work has been supported by a private donation of Trond Mohn C/O Frank Mohn AS, Bergen.
I would also like to thank my fellow students for good times at Geofysen! And last but not least, thanks to Oddbjørn for your encouragement, support and for keeping up my spirits!

Katrine Dale Bjordal
Bergen, May 5, 2006

Contents

Chapter 1

Introduction

South of the Fram Strait-Spitsbergen-northern Norway transect and north of the Greenland-Scotland Ridge is the region that in general is defined as the Nordic Seas. It covers about $2.5 \cdot 10^6$ km^2 or about 0.75 % of the area of the world's oceans (Drange et al. 2005). Atmospheric temperatures are much higher in this region compared to locations at similar latitudes. For the present-day climate, the annual and winter mean temperatures of the central and eastern Nordic Seas are 10 °C and 20 °C higher, respectively, than the zonal means (Drange et al. 2005). These anomalously high temperatures are among others due to prevailing southwesterly, vapor-laden winds and oceanic flow patterns where the Gulf Stream and the North Atlantic Current system maintain a poleward transport of heat.

Despite its limited extent, the region is very dynamic and diverse. The Nordic Seas has a sea floor with complex topography. There are strong atmosphere-ocean transfers of heat, momentum, freshwater and gases, and the typical dynamical length scales are small (Drange et al. 2005). Water masses originating from the North Atlantic and the Arctic Oceans meet here and interact, and sea ice formation takes place in the northern and western part during winter while the region is mainly ice-free during summer.

The combination of the large heat import from the south plus the location between polar and extratropical climate regimes implies that the region is prone to natural climate variations and is especially vulnerable for external forcing, such as global warming for instance (Drange et al. 2005). The Nordic Seas is particularly important for water mass modification and formation and it acts as the major transport route for heat and freshwater between the North Atlantic and the Arctic Ocean. Our understanding of the Nordic Seas is consequently a crucial element in advancing the knowledge of climate dynamics in the northern hemisphere (Drange et al. 2005b).

Due to the anomalously mild climate at these high latitudes, the adjacent land re-

gions of the Nordic Seas have hosted people for untold centuries (Drange et al. 2005b). The activities in the Nordic Seas have increased with time. Today a lot of fisheries and oil drilling take place. During recent years offshore oil-exploration activities have expanded off the continental shelves to deeper waters. The climate debate also takes high priority these days. "Compilations of state-of-the-art climate research are of particular importance for policy makers and governmental bodies to ensure proper, scientifically based knowledge for assessing human-induced global and regional climate change issues, and for conducting optimal timing and scaling of mitigation and adaptation strategies" (Drange et al. 2005b).

The Nordic Seas is obvious important in several ways. Its unique location and in this context its small extent, which allows for accessibility and detailed exploration, are of special importance (Drange et al. 2005b). During the second half of the 19th century oceanographic investigations in the North Atlantic region were initiated and led to significant advances in our knowledge of the sea. The countries in northern Europe, including Russia, were involved in this work (Blindheim & Østerhus 2005). In Norway, Helland-Hansen and Nansen made the pioneering work, which was published in 1909 (Helland-Hansen & Nansen 1909). They described the oceanographic features of the Nordic Seas in such detail and to such precision that it acted as the basic source of information on the general oceanography in the area for many years. This was an active period for oceanographic research in Norway. The Nordic Seas have been further investigated in the 20th century. For a summary of the historical background of research in the Nordic Seas, see Blindheim & Østerhus (2005).

In recent years international scientific cruises are often taking place, and there are several sections that have been repeated regularly. This is, as in the rest of the world, a part of the traditional way of monitoring the ocean. Measurements are usually made from ships or moorings. But there are some disadvantages by this method. It takes a lot of time and it is costly as advanced instruments, skilled technical personnel and research vessels are needed. This is a limiting factor for the quantity for collecting high quality oceanographic data (Mork 2005). The measurements are also dependent of the weather and the sea ice conditions which results in more observations taken during summer than wintertime. Additionally, it can take a long time before the data become available to the scientific community.

In the last decades polar orbiting satellites have been used to monitor the high latitude oceans, notably sea ice concentration and extent, sea surface temperature, wind and wave field. But they have the restrictions that they only monitor the ocean surface. The need for systematic and real time monitoring of the ocean interior has therefore resulted in an increased attempt to use new technology. This is the origin of the in-

ternational Argo project (http://www.argo.ucsd.edu) where the aim is to deploy 3000 free-drifting profiling floats in the worlds oceans, collecting information on the temperature and salinity in the upper 2000 meters (Mork 2005).

During recent decades, modelling of the ocean has developed and improved, and the need for forecast models of the ocean has increased in response to growing offshore activities. TOPAZ (http://topaz.nersc.no) is a forecast model for the Atlantic Ocean developed at the Nansen Center. For model validation, data assimilation and to advance ocean processes understanding, there is a need for remotely sensed data and in situ data. As previously described, in situ data are often irregular in both time and space while the remotely sensed data only provide information from the surface. The Argo floats however provide a continuous and near real-time, in situ data set that will contribute to improvements of forecast models. The plan is to implement assimilation of Argo data in the TOPAZ model.

This study provides an examination of the deep-water currents and the hydrography in the Nordic Seas, obtained by the Argo floats. A comparison of the present TOPAZ model against the Argo data has also been done. Chapter 2 contains a description of the bathymetry and circulation in the Nordic Seas, while the Argo profiling floats and the TOPAZ model are described in chapter 3. Results are given in chapter 4, with trajectories of each Argo float within the Nordic Seas and their temperature and salinity profiles. A brief comparison is done between Argo profiles and measurements obtained at station M. Deep-water currents are estimated from the drift of the Argo floats and the major watermasses in the Nordic Seas are presented in a TS-diagram, with both Argo and TOPAZ data. The discussion of chapter 5 considers the topographic steering of deepwater currents in the Nordic Seas. Comparisons of the TOPAZ model against climatology and Argo data are also discussed. Finally the main conclusions of this study are summarized in chapter 6.

Chapter 2

Description of the investigation area: The Nordic Seas

2.1 Bathymetry

The Nordic Seas consist of the Norwegian, Greenland and Icelandic Seas. Figure 2.1 shows the bathymetry of this area, with names that are mentioned in the text. Bottom contours are drawn for every 500m, and additionally the positions of deployment for all the active Argo floats in the Nordic Seas are indicated.

The Nordic Seas are connected to the Arctic Ocean through the Fram Strait. The Fram Strait is between Greenland and Spitsbergen. It is 650 km wide and has a sill depth of approximately 2600m. Warm Atlantic water flows northwards along the west coast of Spitsbergen into the Arctic Ocean and cold water and ice are flowing south along the east coast of Greenland. The Fram Strait is the deepest connection with the Arctic Oceans (Blindheim & Østerhus 2005).

At the northeastern margin of the Nordic Seas, between Svalbard and northern Norway, there is an opening to the Barents Sea. South of the Bear Island is the Bear Island Trough where a substantial part of the water exchanges between the Nordic Seas and the Barents Sea takes place (Blindheim & Østerhus 2005). The trough is about 400m deep.

South of the Fram Strait is the Greenland Sea limited by Greenland at the west and the mid-ocean ridge at the east. The Greenland Sea consists of two basins, the Boreas Basin to the north and the Greenland Basin to the south. The Greenland Basin is the larger and deeper one with 3400 to 3600m depth. The Boreas Basin is smaller and shallower with depths around 3200m. The Greenland Fracture Zone separates them (Perry 1986).

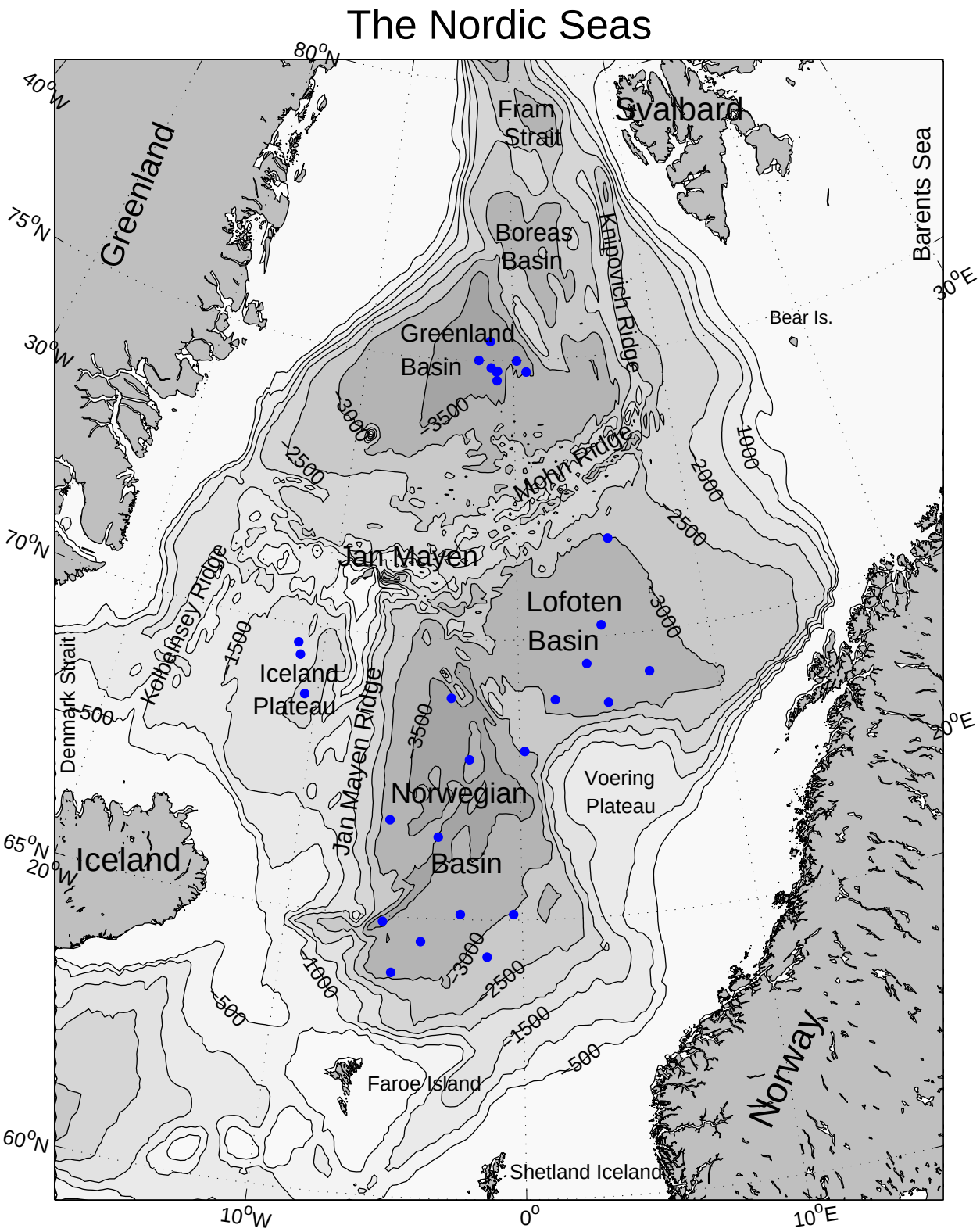

Figure 2.1: ***Main bathymetric features in the Nordic Seas. The blue dots indicate the positions of deployment for all the active Argo floats in this area.***

The mid-ocean ridge is a prominent topographic feature and consists of three main parts. The Knipovich Ridge extends southward from the Fram Strait, with its shallower crests being about 1000m deep. Between approximately 73.5 °N, 8 °E and Jan Mayen, the Mohn Ridge is located with depths ranging between 1000-2000m. It has a rather complex topography and is characterized by many isolated bathymetric features. At the latitude of Jan Mayen, the Jan Mayen Fracture Zone cuts through the mid-ocean ridge. South of this zone is the Kolbeinsey Ridge that extends southward to the North Icelandic shelf (Vogt 1986).

The Icelandic Sea is bounded by Iceland to the south and the Jan Mayen Fracture Zone to the north. The Iceland Plateau is east of the Kolbeinsey Ridge. The Jan Mayen Ridge, at the eastern margin of the plateau, extends southward from Jan Mayen. There is a small basin more than 2200m deep at the west of this ridge.

The Norwegian Sea is to the east of the mid-ocean ridge. It consists of the Lofoten Basin, the Norwegian basin and the Vøring Plateau as the main topographic features. The Vøring Plateau is west of the continental slope off the Norwegian coast. The Norwegian Basin extends northward from the Iceland-Faroe Ridge and is limited by the Norwegian continental shelf, the Vøring Plateau and the Jan Mayen Ridge. It is the deepest and largest basin in the Nordic Seas. The floor is mainly between 3200 and 3600m, with a maximum depth that exceeds 3800m in a narrow trough around 65 °N, 5 °W. To the north of the Norwegian Basin and the Vøring Plateau and southeast of the Mohn Ridge is the Lofoten Basin. This is smaller and shallower with depths around 3200m (Blindheim & Østerhus 2005).

To the south, the Greenland Scotland Ridge separates the Nordic Seas from the North Atlantic Ocean. The ridge consists of three gaps. Starting at the western end, between Greenland and Iceland, the Denmark Strait is located with a sill depth of about 620m. The second gap, between Iceland and the Faroe Islands, is the Iceland-Faroe Ridge with maximum depths of 400-500m. The topography between the Faroes and Scotland is more complex. Here the main entrance to the Nordic Seas is through the Faroe-Shetland Channel, which has a sill depth of about 600m (Hansen & Østerhus 2000). Between the Shetland Island and the southwestern Norway there is an opening to the North Sea.

2.2 Circulation

Warm and saline North Atlantic water flowing northwards, mainly on the eastern side, and colder Polar Water flowing southwards with the East Greenland Current (EGC) on the western side dominates the large-scale surface circulation in the Nordic Seas

(Blindheim et al. 2000). Figure 2.2 shows the schematics of the circulation here. The Atlantic water enters the Nordic Seas by the North Icelandic Irminger Current through the Denmark Strait, by the Faroe Current across the Iceland-Faroe Ridge and by the Atlantic Inflow through the Faroe-Shetland Channel. Parts of the Atlantic Water are transported northwards with the Norwegian Atlantic Current (NWAC) to the Barents Sea and the Arctic Ocean (Hansen & Østerhus 2000). Most of the remaining parts of the Atlantic Water continue into the Norwegian and the Lofoten Basin.

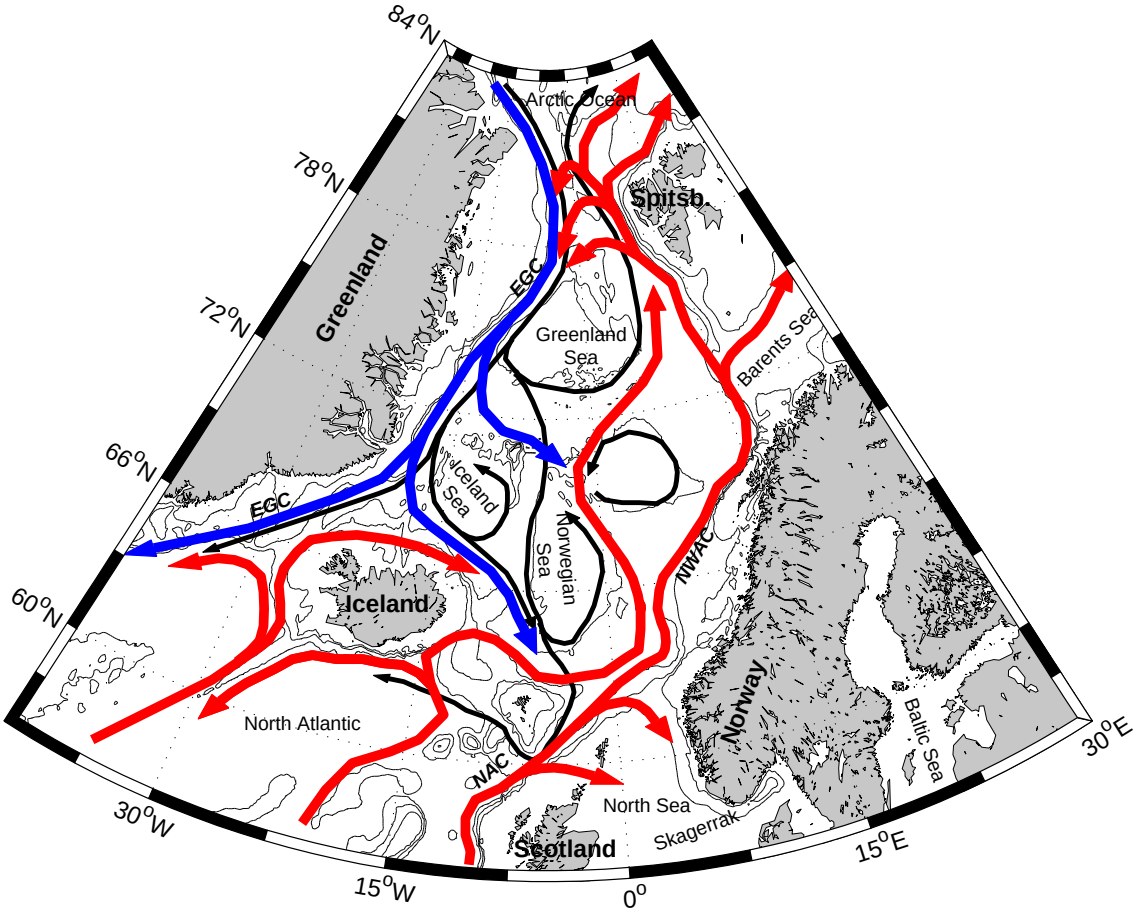

Figure 2.2: ***Sketch of the flow of the Nordic Seas. The thick arrows represent the surface flow of Atlantic Water (red) and Polar Water (blue), while the thin black arrows indicate the flow of intermediate and deep waters. Figure is taken from Eldevik et.al. (2005).***

The southward flowing EGC carries cold and fresh Polar surface waters, including sea-ice (Aagard & Carmack 1989), intermediate and deep waters from the Arctic Ocean (Rudels et al. 1999), Atlantic Water that has deflected westwards from the West Spitsbergen Current and waters of Atlantic origin that has circulated the Arctic Ocean (Recirculating Atlantic Water). Due to topographic features, parts of these waters

divert into the Greenland and Boreas basins (Blindheim & Østerhus 2005). The first main branch of the EGC is the Jan Mayen Current (JMC), which brings the water masses into the cyclonic circulation in the Greenland Sea. The second main branch, the East Icelandic Current, is further south. It carries watermasses from the EGC into the Iceland and the Norwegian Seas (Buch et al. 1996). The remaining water leaves the Nordic Seas through the Denmark Strait (Blindheim et al. 2000).

Additionally some dense bottom water that is formed in the Barents Sea enters the Norwegian Sea through the Bear Island Trough (Blindheim & Østerhus 2005).

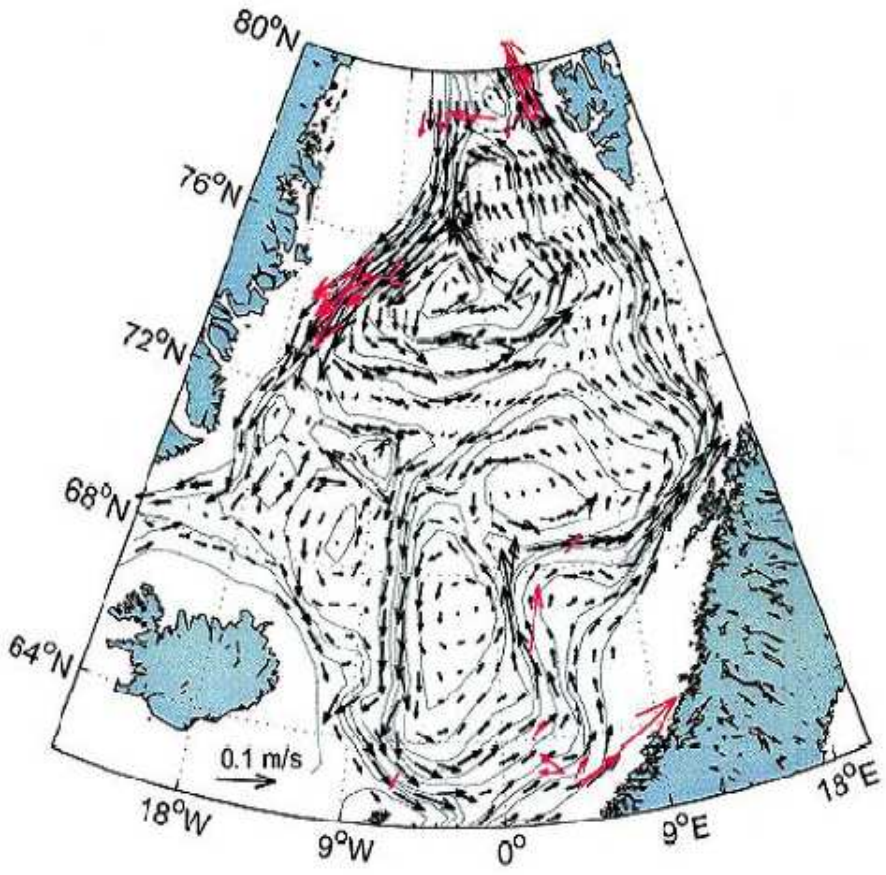

Figure 2.3: ***Modeled bottom geostrophic velocities (black arrows) and observed near-bottom currents (red arrows) for the Nordic Seas. Figure is taken from Nøst and Isachsen (2003).***

The surface flow in the Nordic Seas has been well investigated through several drifter measurements over the past decade (Jakobsen et al. (2003), Orvik & Niiler (2002), Poulain et al. (1996)). The intermediate and deep water flows are less known, but

according to Eldevik et al. (2005), they are generally in the same direction as the surface flow and there is also a cyclonic circulation within the subbasins in the Nordic Seas. This general picture (see Figure 2.3) is based on diagnostic calculations using climatological hydrography and wind-stress curl as input (Nøst & Isachsen 2003) and on rather few measurements in deep water (Hansen & Østerhus 2000).

As defined by Blindheim & Østerhus (2005), the major water masses in the Nordic Seas, with their potential temperature, salinity and a short description of their locations are listed in Table 2.1.

Water mass	Potential temp. (°C)	Salinity
Canadian Basin Deep Water (CBDW) flows across the Lomonsov Ridge north of Greenland and enters the Nordic Seas between approximately 1500 and 2000m over the Greenland Slope.	$-0.8 < \theta < -0.5$	> 34.92
Eurasian Basin Deep Water (EBDW) occupies the deeper strata of the Eurasian Basin in the Arctic Ocean. Between approximately 2000m and the sill depth in the Fram Strait (∼2500m) EBDW enters the Nordic Seas over the Greenland Slope.	$-0.7 < \theta < -0.9$	34.92-34.93
Greenland Sea Arctic Intermediate Water (GSAIW) is formed in the Greenland Sea by convection but is less dense than older deep water. The properties entered represent the 1990s.	$-0.9 < \theta < -0.5$	34.86-34.89
Greenland Sea Deep Water (GSDW) is a mixture of deep water formed locally by convection during cold winters, and deep waters deriving from the Arctic Ocean.	< 0	34.88-34.90
Iceland Sea Arctic Intermediate Water (ISAIW) is partly formed in the northern/central Iceland Sea by winter convection and partly derives from similar intermediate waters in the Greenland Sea.	< 1	34.7-34.9
Iceland Sea Deep Water (ISDW) is similar to NSDW but has slightly higher salinity due to admixture of CBDW.	~ -1	34.91-34.92
Irminger Sea Water (ISW) derives from the North Atlantic Current and is carried into the Nordic Seas by the North Icelandic Irminger Current. Properties given are those in the northern Irminger Sea.	5-7	35.05-35.10
Modified East Icelandic Water (MEIW) is an intermediate water in the southwestern Norwegian Sea characterised by waters from the East Icelandic Current and the North Iceland Irminger Current.	1-3	34.6-34.9
Modified North Atlantic Water (MNAW) has its origin in the North Atlantic Current. It flows through the Iceland Basin and across the Iceland-Faroe Ridge into the Nordic Seas.	7.0-8.5	35.1-35.3
North East Atlantic Water (NEAW) enters the Nordic Seas through the Faroe-Shetland Channel. It derives mainly from the slope current to the west of the British Islands.	9.0-10.5	35.3-35.45
Norwegian Sea Arctic Intermediate Water (NSAIW) advects from the Iceland and Greenland Seas into the Norwegian Sea, where it occurs in a layer identified by a salinity minimum between the upper layers, composed mainly of Atlantic Water, and the deep water.	$-0.5 < \theta < 0.5$	34.7-34.9
Norwegian Sea Deep Water (NSDW) fills the Norwegian Sea beneath the NSAIW.	< 0.5	34.91
Polar Intermediate Water (PIW) forms a temperature minimum underneath the upper waters of the East Greenland Current.	< 0	34.4-34.7
Recirculating Atlantic Water (RAW) is water of Atlantic origin that has circulated into the East Greenland Current from the West Spitsbergen Current and the Atlantic layer in the Arctic Ocean.	0-2	34.9-35.0

Table 2.1: ***Major Water Masses in the Nordic Seas Defined by Potential Temperature (θ) and Salinity. Table is taken from Blindheim and Østerhus (2005).***

Chapter 3

Instruments and Methods

3.1 Argo profiling floats

3.1.1 Instrumentation

Argo uses robotic floats that spend most of their life passively drifting below the ocean surface. The drifting depth is chosen, usually at 2000 meters depth. The floats have a pressure case made of aluminium tube that is about 1.3m long and has a diameter at about 20cm. They weigh about 40kg. Figure 3.1 shows a picture of an Argo float. On the top is an antenna to communicate with the satellites that fix the float's position and transmit the data. Also on the top are the temperature and salinity sensors. At the bottom of the float in a protective cover is a bladder that is connected to the inside of the float. The floats are designed so that with the bladder empty they have the same density as seawater at the depth at which they drift. They are also designed to be less compressible than seawater. This keeps them stable at depth.

The floats are put in the ocean from ships or aircrafts and sink to the reference depth. After 10 days oil is pumped from the pressure case into the bladder. The bladder inflates and the volume increases. As the mass remains the same, its density decreases and this drives the float to the surface. During the ascent it measures pressure, temperature and salinity, i.e. it makes profiles. At the surface the float is positioned after an ascent and before a descent by satellites and it transmits its temperature/salinity profile. The distance and time between two sequences of ascents can easily be utilized to estimate the velocity and direction of the drift of the float. Ignoring the error due to drift during the ascent and at the surface, we can assume that the drift of the float is similar to the currents at their reference depth. These velocities are called Langrangian, which means the actual velocity of a parcel as it moves relative to the earth. We follow the movement of the float instead of measuring the velocity at a fixed position. The float positions are accurate to about 100 meters depending on the number of satellites

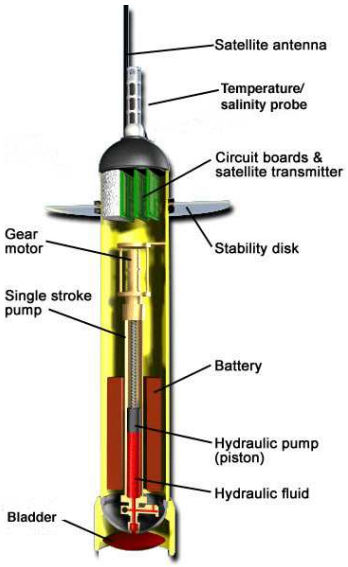

Figure 3.1: ***Argo float***

within range and the geometry of their distribution. The floats must spend between 6 and 12 hours at the surface to guarantee error free data reception and location in all weather conditions. Thereafter the bladder deflates as oil is pumped back into the pressure case. The density of the float increases and it sinks back to the reference depth. It repeats the cycle after 10 days. Each float must deliver high-quality data while cycling over 200 atmospheres and through a temperature range that may reach 30 °C. Figure 3.2 shows the typical operation mode of an Argo float.

The floats are powered by batteries. Many use manganese/alkali batteries like you can buy in shops. Some floats use higher-powered lithium batteries. The floats are designed to do about 140 cycles and so should last almost 4 years. The lifetime depends on the depth to which they profile and the surface water density in which the float is operating. If the surface water has low density, more oil must be pumped to drive the float to the surface.

The three float types in use are the PROVOR built by MARTEC in France in close collaboration with IFREMER, the APEX float produced by Webb Research Corporation, USA and the SOLO float designed and built by Scripps Institution of Oceanography, USA.

3.1.2 Global distribution

The first Argo floats were deployed in 2000. The aim of this project is to have 3000 Argo floats globally distributed. At present (January 2006) there are about 2200 floats

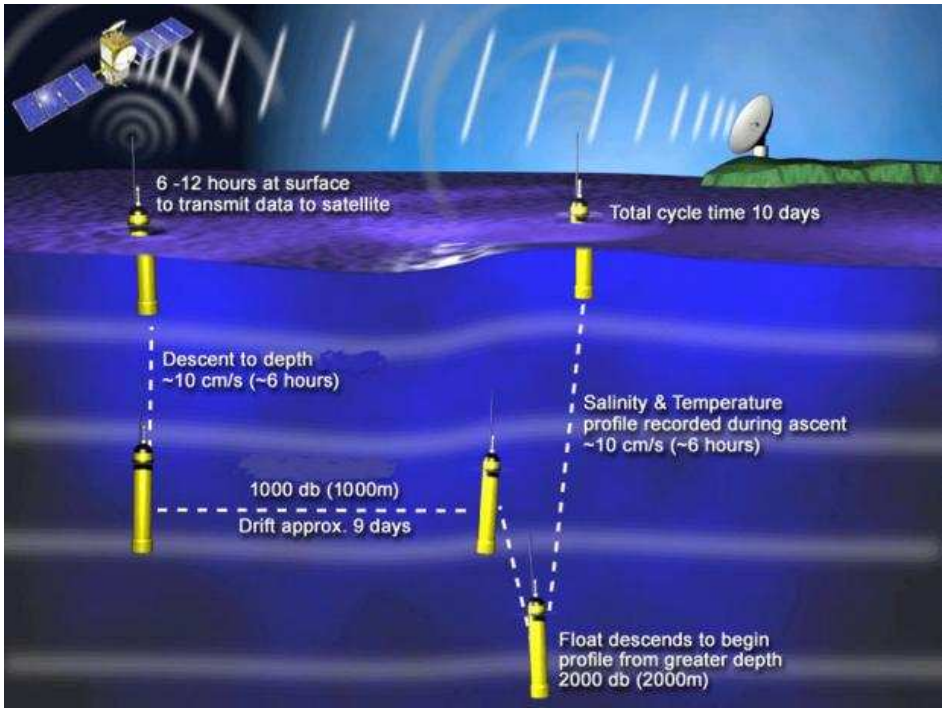

Figure 3.2: ***The typical operation mode of an Argo float.***

operational. The final Argo array will yearly provide about 100 000 vertical profiles of temperature and salinity. It will probably be complete in 2006/2007. Figure 3.3 shows a map with all the Argo floats currently (January 2006) distributed in the world's oceans.

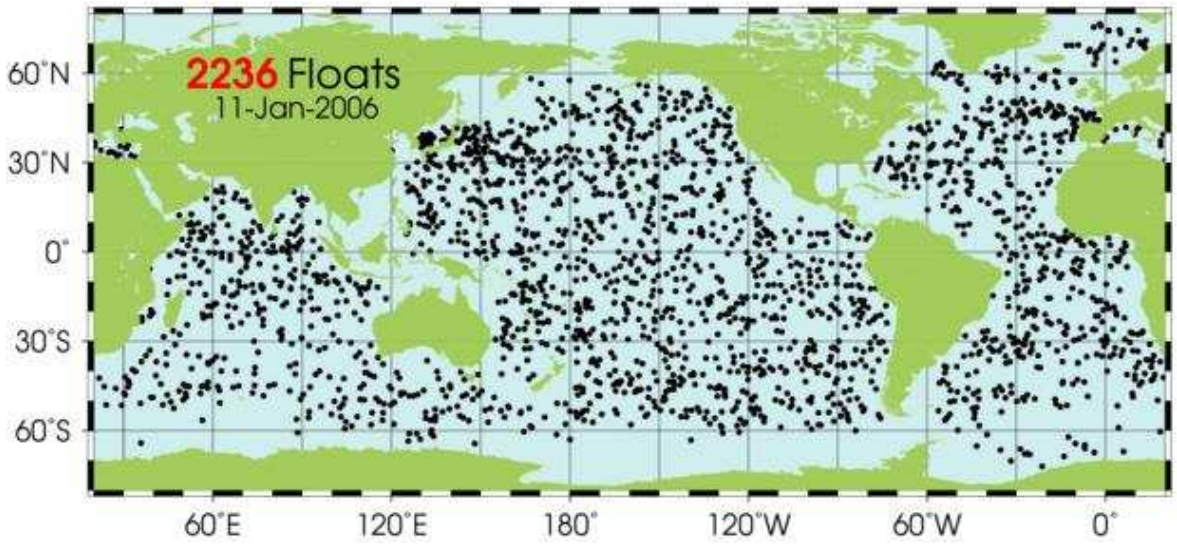

Figure 3.3: ***Global distribution of Argo floats (January 2006).***

Any agency, country or consortium can take place in the Argo program, but all data shall be freely available for everyone. 19 countries have so far contributed with Argo floats; Australia, Canada, China, Denmark, France, Germany, India, Ireland, Japan, Korea, Mauritius, Netherlands, New Zealand, Norway, Russia, Spain, UK, USA and the European Union. Funding mechanisms differ widely between countries and involve over 50 research and operational agencies. The contributions range from a single float to the U.S. contribution, which is about 50% of the global array.

Several other countries including South Africa, Indonesia, and Chile have contributed greatly with float deployments. Wider participation in Argo by many nations and research groups is encouraged either through float procurement, logistical support for float deployment or through analysis and assimilation of Argo data.

3.1.3 Argo data

An important issue about Argo is the fact that the data are free to anyone to use. As a contributor, one must agree that any data collected must be made available immediately and without restrictions (Gould 2002*b*).

For most Argo floats the data are transmitted via the ARGOS data transmission system. The satellites of the ARGOS system look down on all Argo transmitters within a 5000-km-diameter circle and they relay data to ground stations from their altitude of 850 km.

Argo data are processed and distributed through a network involving different actors (Gould 2002*a*). The first step is when data are transmitted by satellites to National Centers. These are also called Data Assembly Centers - *DAC*s. Here the data are processed and qualified before further distribution. Generally they are responsible for converting the data stream from each float to profile and drift information. The data are then made available for the users through 3 different routes. One is directly from the DACs to operational centers, using the GTS (Global Telecommunication System). At the same time, data are also sent to Global Data Centers, GDACs, within 24 hours. These are distributions points on Internet and there are two of them. The American Monterey site is located at *www.usgodae.org/argo/argo.html* and the French Coriolis site is located at *www.coriolis.eu.org/cdc/argo.htm*. To gain the best data one request to centralize this function and get all users to obtain their data from the GDACs. The data can be downloaded by ftp, http and Live Access Server (LAS). Both servers are coordinated daily to ensure consistency between them. This is the second route.

The same data are sent from DACs to PIs and Delayed Mode Centers. The PI, Princi-

pal Investigator, is the scientist who deploys the floats and who is the main responsible for the quality of the data. Here one carries out quality checks, testing and calibrations to ensure high quality data. Within 5 months the data are sent back to the DACs and further on to the GDACs as delayed mode data (Carval et al. 2006).

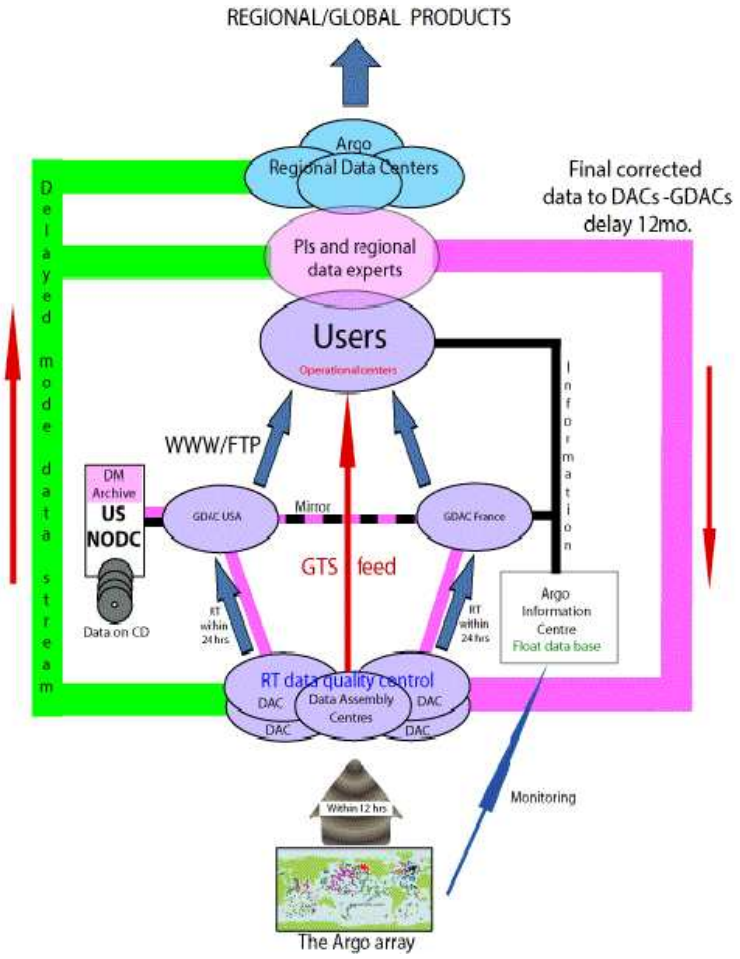

Figure 3.4: ***Argo data flowchart.***

The third route where data are available is from an archived data set at the US NODC, National Oceanographic Data Center. This is a long term archive of all the Argo data and it is possible to get the data on CDs or DVDs for users without Internet access. It also works as a backup for the GDACs.

There are also Regional Data Centers, which are responsible for quality control on float data collected in specified regions. They get the data from National and Global Data Centers. Validation through more rigorous quality control takes place and they also derive Argo data products and services.

AIC, the Argo Information Center, is responsible for the international technical coordination of Argo. They don't distribute nor archive data, but shall provide information on the Argo program and guide the users to the GDACs and regional products. The center is established in Toulouse, France. Figure 3.4 is a schematic overview of the Argo data flow.

3.1.4 Argo floats in the Nordic Seas

At present (January 2006) there are 28 active floats in the Nordic Seas. Three of them have stopped profiling, but they are still considered active, as they have been for most of the period I have worked on this thesis. The Institute of Marine Research (IMR), Bergen, Norway, is responsible for 9 Argo floats while the rest of the floats are German, deployed by the University of Hamburg (UoH). Although the main focus is on the Norwegian floats, the others are also to some extent studied. Table 3.1 shows an overview of the floats considered in this thesis, with date of deployment, date of the latest profile according to this data set, the drifting region, profile and parking depths. Note that all the Norwegian floats are drifting at 1500m depths while the German floats are drifting at depths of either 1000m or 1500m. The floats will for the rest of the thesis be referred to as the three last numbers of their name. E.g. float 6900215 will be named 215.

Name	Institution	Date of deployment	Date of latest profile of this data set	Region	Profile depth	Parking depth
6900215*	IMR	21.06.02	23.10.05	Norwegian Sea	1500m	1500m
6900216	IMR	21.06.02	23.10.05	Norwegian Sea	1500m	1500m
6900217*	IMR	10.06.02	05.04.05	Norwegian Sea	1500m	1500m
6900218	IMR	14.08.03	01.11.05	Norwegian Sea	1500m	1500m
6900219	IMR	14.08.03	01.11.05	Norwegian Sea	1500m	1500m
6900220	IMR	15.08.03	23.10.05	Norwegian Sea	1500m	1500m
6900221	IMR	14.08.03	21.10.05	Norwegian Sea	1500m	1500m
6900222	IMR	14.08.03	01.11.05	Norwegian Sea	1500m	1500m
6900223	IMR	14.08.03	22.10.05	Norwegian Sea	1500m	1500m
6900303	UoH	18.10.04	03.10.05	Greenland Sea	2000m	1000m
6900304	UoH	18.10.04	03.10.05	Greenland Sea	2000m	1000m
6900305	UoH	18.10.04	03.10.05	Greenland Sea	2000m	1000m
6900306	UoH	18.10.04	04.10.05	Greenland Sea	2000m	1000m
6900307	UoH	19.10.04	04.10.05	Greenland Sea	2000m	1000m
6900328	UoH	12.03.05	08.10.05	Norwegian Sea	2000m	1500m
6900329	UoH	12.03.05	08.10.05	Norwegian Sea	2000m	1500m
6900330	UoH	13.03.05	09.10.05	Norwegian Sea	2000m	1500m
6900331	UoH	13.03.05	09.10.05	Norwegian Sea	2000m	1500m
6900334*	UoH	08.03.05	04.10.05	Norwegian Sea	2000m	1500m
6900335	UoH	08.03.05	04.10.05	Norwegian Sea	2000m	1500m
6900336	UoH	08.03.05	04.10.05	Norwegian Sea	2000m	1500m
6900339	UoH	03.10.05	11.01.06	Greenland Sea	2000m	1000m
6900340	UoH	17.10.05	05.01.06	Norwegian Sea	2000m	1000m
6900341	UoH	03.10.05	11.01.06	Greenland Sea	2000m	1000m
6900342	UoH	03.10.05	01.01.06	Greenland Sea	2000m	1500m
6900343	UoH	16.10.05	04.01.06	Iceland Sea	1300m	1000m
6900344	UoH	16.10.05	04.01.06	Iceland Sea	1300m	1000m
6900345	UoH	16.10.05	04.01.06	Iceland Sea	1300m	1000m

* These floats are per January 2006 not operating any more.

Table 3.1: ***Active Argo floats in the Nordic Seas.***

3.2 TOPAZ

TOPAZ stands for 'Towards an Operational Prediction system for the North Atlantic European coastal Zones.' It is an operational system for the Atlantic and the Arctic Ocean based on HYCOM - the Miami 'Hybrid Co-ordinate Ocean Model,' that is developed from the Miami Isopycnic Coordinate Ocean Model (MICOM; Bleck & Smith (1990)) by Bleck (2002). HYCOM is a 'state of the art' ocean general circulation model (OGCM) where current velocity, water temperature and salinity data are provided. HYCOM can operate in both hindcast and forecast mode (Bertino & Evensen 2003). TOPAZ aims at providing real-time forecasts for both the physics and ecology of the North Atlantic Ocean.

The monitoring and forecasting system covers the whole Atlantic Ocean from 60 °S up to, and including, the Arctic Ocean (see Figure 3.5). A model grid is constructed, based on 'conformal mapping' (Bentsen et al. 1999), with horizontal grid spacing between 18 and 35 km. HYCOM can be run at basin scale to represent circulation of large oceanic water masses, but the system can also provide boundary forcing for nested fine resolution models of regions of particular interest. The water column is divided in 22 layers of varying depths (Bertino et al. 2004).

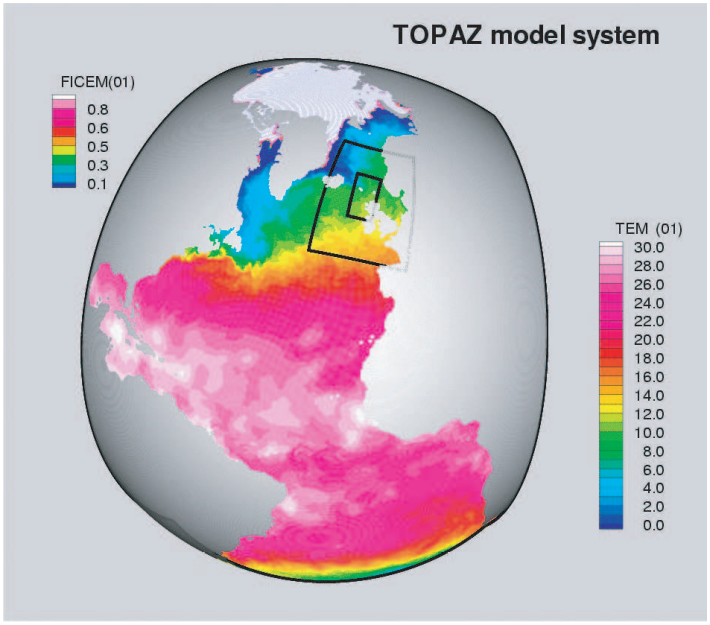

Figure 3.5: ***The model domain used in the TOPAZ real time experiment. The plot shows surface temperature and ice concentration. (From Bertino et.al. 2004.)***

For ocean models there are mainly three traditional vertical coordinate choices. Z-level coordinates have layers at fixed depths below sea surface, terrain-following coordinates

have layers at a fixed proportion of the total water depth and isopycnic coordinates have layers of constant density and varying thickness. By themselves they are not optimal everywhere in the ocean, but each type of coordinates have their advantages. Ideally, an ocean model should retain its water mass characteristics for centuries (a characteristic of isopycnic coordinates), have high vertical resolution in the surface mixed layer for proper representation of momentum transfer from the atmosphere to the ocean, thermodynamic and biochemical processes (a characteristic of z-level coordinates), maintain sufficient vertical resolution in unstratified or weakly-stratified regions of the ocean, and have high vertical resolution in the coastal regions (a characteristic of terrain-following coordinates). A hybrid model, like HYCOM, combines all the three coordinates to benefit from the advantages of the different types. In the open, stratified ocean the hybrid coordinate is isopycnal, but in shallow coastal regions it smoothly reverts to a terrain-following coordinate. In the mixed layer and/or unstratified seas it reverts to z-level coordinates.

The model ocean dynamics are driven by three atmospheric forcing fields; surface wind velocity, atmospheric pressure and air temperature fields. Climatology is used for initializing the model, and HYCOM uses the GDEM (Generalized Digital Environmental Model) data (Teague et al. 1990) for this purpose. The spin up time is 5 years.

In the TOPAZ project HYCOM is coupled to a marine ecosystem model and a model for sea ice. TOPAZ involves advanced data assimilation where the Ensemble Kalman Filter (EnKF) is the scheme used (Evensen (1994), Evensen (2003) and Brusdal et al. (2003)). Data that are assimilated are satellite observed Sea Level Anomaly (SLA) from altimetry, Sea Surface Temperature (SST) from infrared radiometers and Sea-ice concentrations from passive microwave imaging. Soon Coriolis in-situ data (Argo) will be assimilated as well.

Operational data are archived and are available for subsequent use as profiles, spatial fields and point-specific time series. Archived data are used in this thesis. The model run that is used started the 1^{st} of January 2005. Due to changes in the format of the data files, only data until the 20^{th} of September 2005 are used.

Chapter 4

Results

4.1 Measurements obtained by Argo in the Nordic Seas

A presentation of the data obtained by the Argo floats in the Nordic Seas will be given in this chapter. Figure 2.1 shows all the active floats in this area. The blue dots indicate the positions of deployment for each float.

4.1.1 Trajectories

The trajectories of each Argo float in the Nordic Seas will now be displayed and examined. Table 3.1 gives an overview of all the floats, including information on dates of deployment and dates of the last obtained profile (also indicated below each trajectory figure). On the trajectory figures (Figures 4.1 - 4.7) the blue dots indicate where the profiles have been taken, while the blue lines in between, connecting these points, are the trajectories for the subsequent 10 days drift period. The green circles mark the position of the float deployments while the red circles mark the position where the last profile of this data set was taken. Bottom contour lines are drawn every 500m.

NORWEGIAN BASIN
Three of the Norwegian Argo floats, 215-217, were deployed in the middle of the Norwegian Basin during June 2002, see Figure 4.1a-c. In August 2003, IMR deployed three more floats, 221-223, in the southern part of the Norwegian Basin, as shown in Figure 4.1d-f. These floats have been drifting for well over three and two years respectively, according to this data set. They have in common a cyclonic drift in the main and are quite close connected to the isobaths. Except from float 223, all the floats stay within the Norwegian Basin all the time.

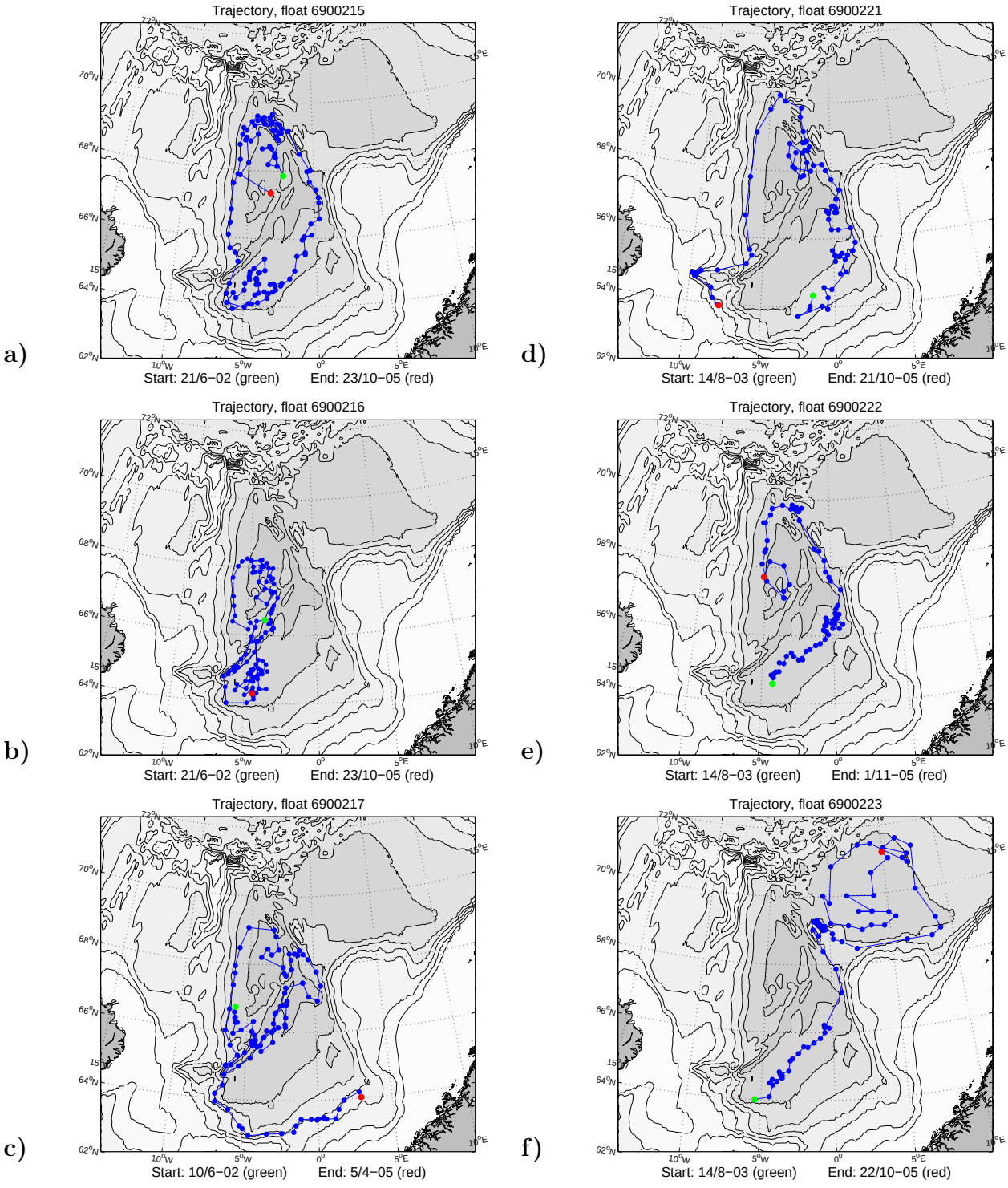

Figure 4.1: ***Trajectories of the Norwegian Argo floats deployed in the Norwegian Basin. Parking depth is 1500m.***
a) Float 215 b) Float 216 c) Float 217 d) Float 221 e) Float 222 f) Float 223.

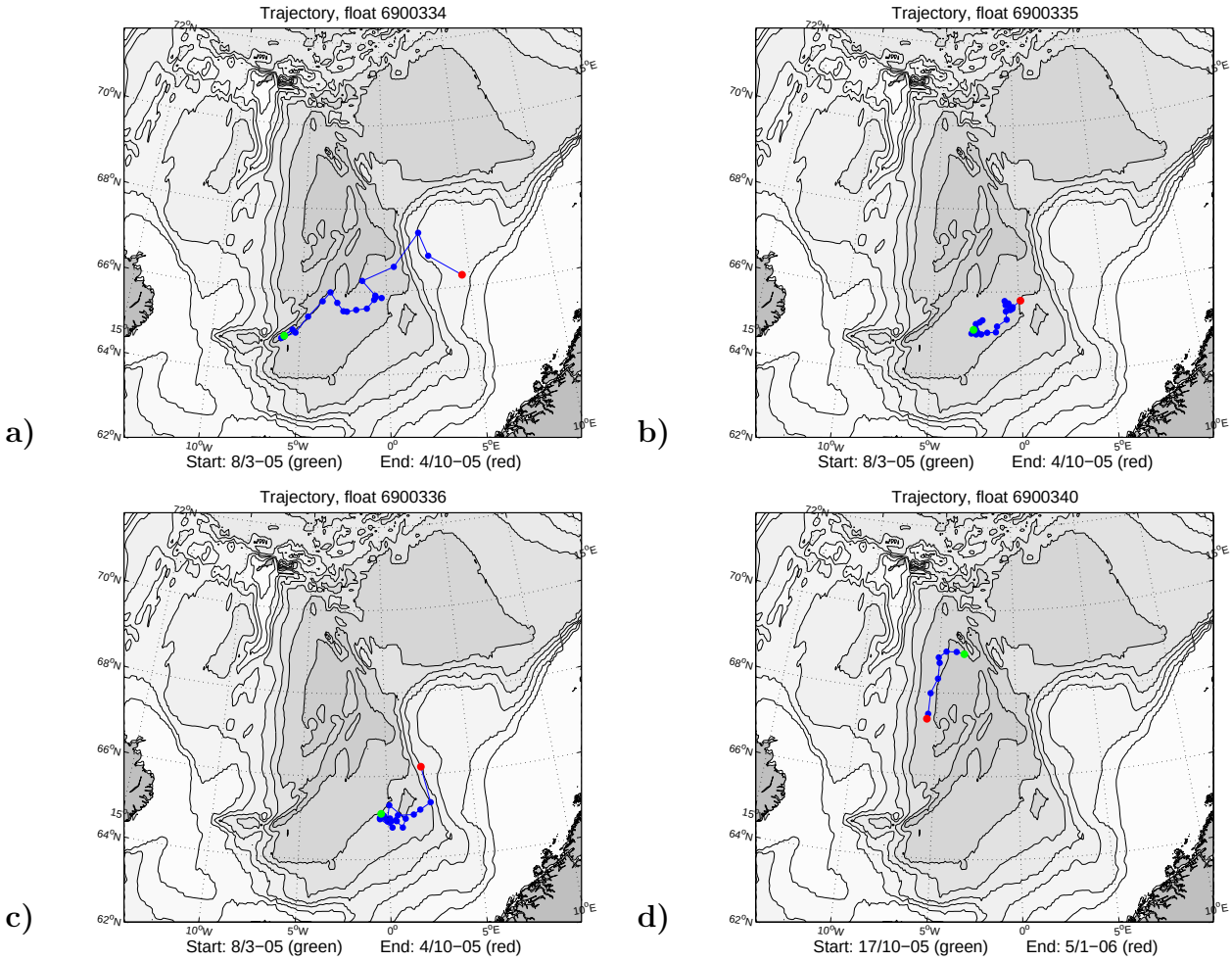

Figure 4.2: ***Trajectories of the German Argo floats deployed in the Norwegian Basin: a) Float 334 b) Float 335 c) Float 336 d) Float 340. Parking depth is 1500m, except float 340 (d), which has a parking depth of 1000m.***

All the floats do follow the 2500-3000m isobaths to a certain degree. Float 216 and 217 (Figure 4.1b and c) are partly trapped above the deepest areas of the basin. These floats follow the 3500m isobath in a southwest-northeast direction as clearly seen from a point around 6 °W, 65 °N (a blow up of the area can be seen in Figures 5.1a and b). Float 223 (Figure 4.1f) leaves the Norwegian Basin and moves into the Lofoten Basin. It follows approximately the same drift as float 222 (Figure 4.1e) during the first half of the drifting period, although slightly further to the north after passing 67 °N. But instead of continuing the cyclonic drift around the Norwegian Basin, it veers off to the east at 1 °W, 69 °N. Another notable feature is the small chaotic movements of float 222 (Figure 4.1e) around 0 °E, 66 °N. A small trace of this can also be seen for float 215, while the path of float 221 makes a strange turn in this area. There is no trace of this chaotic drift for float 223 (Figure 4.1f), but there is a lack of data for a 40-days

period at this location. Hence it is likely that the actual movement is more chaotic than it looks like on the figure.

Notice the large distances between each profile as float 221 (Figure 4.1d) is drifting southwards along the western part of the basin. It has about twice the speed, and the track of float 221 is a bit more to the west compared to the other floats at this distance. The topography gradients are larger here, compared to the gradients slightly further east.

Three German floats, 334-336 (Figure 4.2a-c) were deployed in the southern part of the Norwegian Basin during March 2005, and float 340 (Figure 4.2d) was deployed in the northern part in October 2005. The latter has been drifting for just a few months in this data set, but still the trajectory indicates similar circulation pattern as the other floats in the same area, float 215, 217 and 222. The other three German floats have been in the ocean for about half a year, according to this data set. They are drifting northeastwards, pointing to a cyclonic circulation, but the drifting period is too short to say for sure. Float 334 (Figure 4.2a) is an exception as it from the point at 2 °E, 67 °N leaves the Norwegian Sea and moves across the Vøring Plateau.

LOFOTEN BASIN

In the Lofoten Basin, three Norwegian floats, 218-220 (Figure 4.3a-c) were deployed during August 2003. Float 218 was actually deployed at the northeastern end of the Norwegian Basin, but it drifted along the northern edge of the Vøring Plateau and into the Lofoten Basin at once. These three floats provide data for more than two years. A cyclonic circulation around the basin can be seen here as well, strongly connected to the isobaths. On the average, the floats spend about 15 months completing one circulation around the basin. As float 219 (Figure 4.3b) has finished one and a half circulation, it leaves the Lofoten Basin and moves into the north of the Norwegian Basin. As already emphasized, float 223 (Figure 4.1f) moves into the Lofoten Basin after some drifting in the Norwegian Basin. It makes one circulation around the Lofoten Basin, following the 3000m isobath, until it moves into the middle of the basin and passes across it. On Figures 4.3a-c all three floats show some chaotic movements in the area between $10 - 15$ °E and $69 - 71$ °N. The depths here are 2500-3000m. There are two long legs in the trajectory figures, from 0 to 9 °E at 69 °N in Figure 4.3a and from 11 °E, 70 °N to 7 °E, 72 °N in Figure 4.3c. Both are due to missing data during a 40 days period. Note that all the Norwegian floats are drifting at 1500m depths.

The German floats that are drifting in the Lofoten Basin, float 328-331 (Figures 4.4a-d) were deployed in March 2005 and have data from about half a year. The three first ones

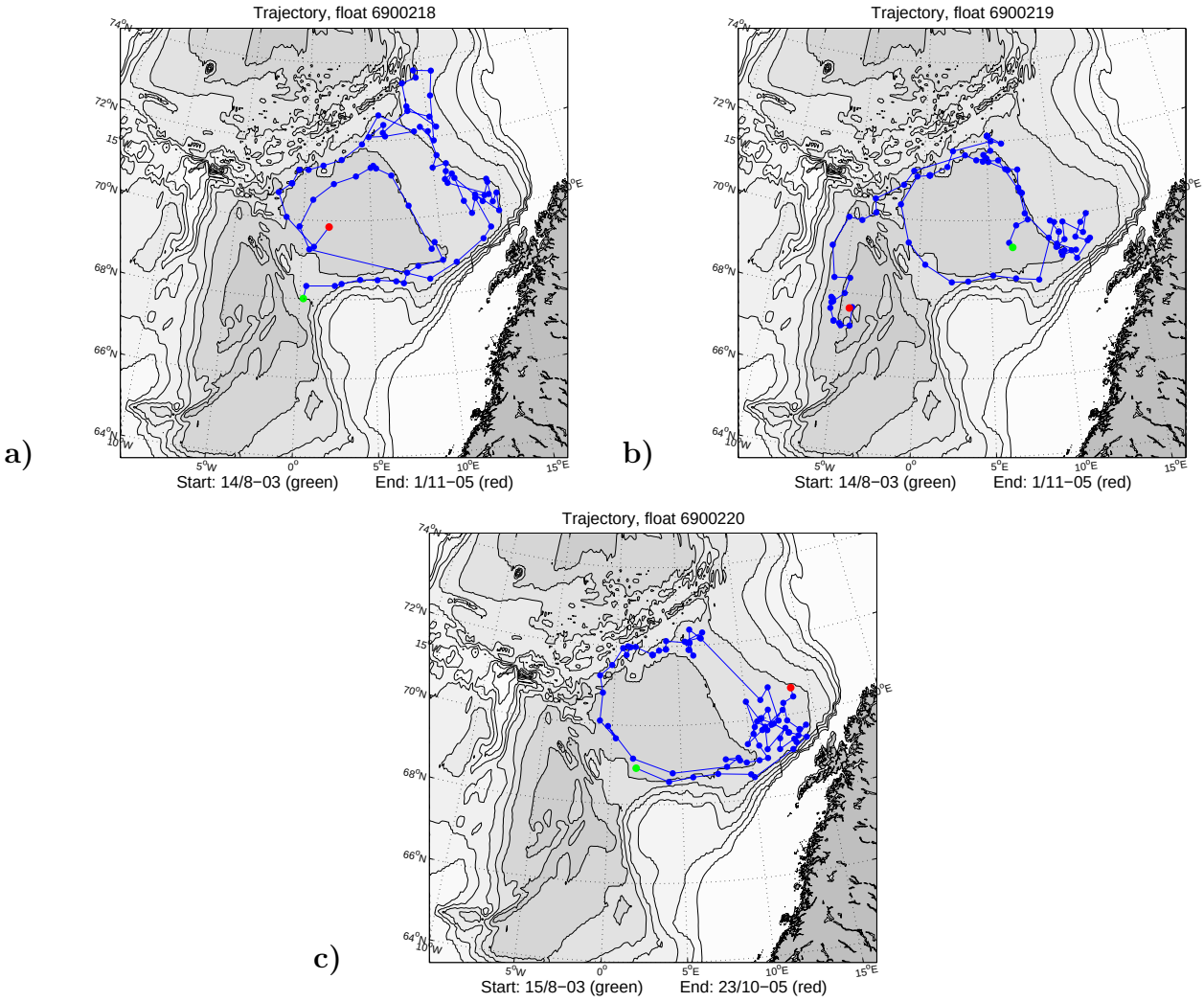

Figure 4.3: ***Trajectories of the Norwegian Argo floats deployed in the Lofoten Basin. Parking depth is 1500m. a) Float 218 b) Float 219 c) Float 220.***

are mainly drifting in the middle of the basin, apparently at random. No pronounced cyclonic circulation is observed, as opposed to the previously described floats drifting at the outer part of the basin. The latter, float 331 (Figure 4.4d) has a seemingly random drift at the north of the Lofoten Basin. The parking depths are the same as for the Norwegian floats in the Lofoten Basin, 1500m.

GREENLAND SEA

During October 2004 five German floats, 303-307 (Figures 4.5a-e), were deployed in the Greenland Basin, drifting at 1000m depths. This data set contains data for about one year. The circulation is all in all cyclonic, although disordered in some areas. This

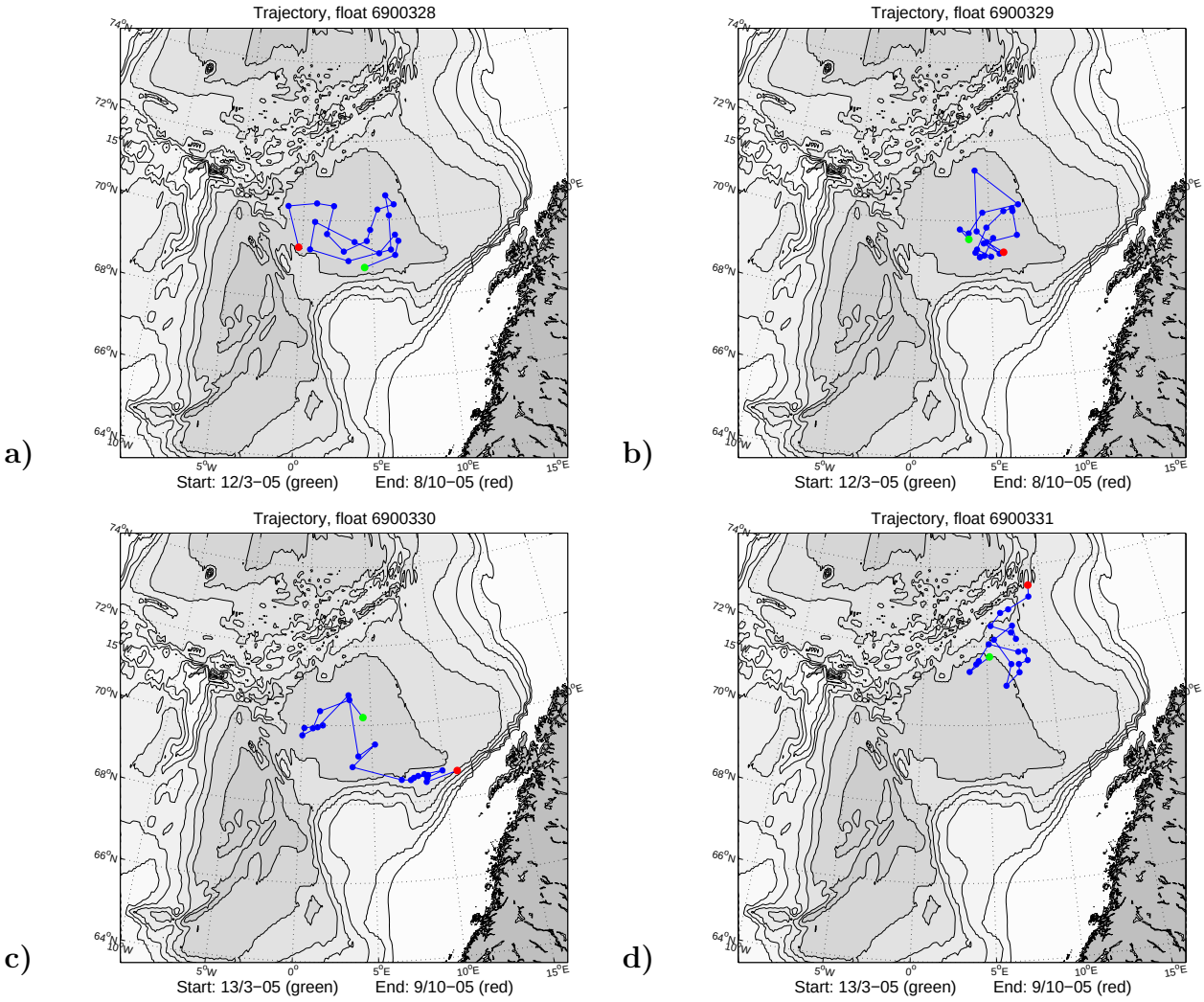

Figure 4.4: ***Trajectories of the German Argo floats deployed in the Lofoten Basin, with parking depth at 1500m:***
a) Float 328 b) Float 329 c) Float 330 d) Float 331.

can particularly be seen in the middle of the Greenland Basin in Figure 4.5e. Floats 303, 305 and 307 remain all the time in the Greenland Basin, while floats 304 and 306 (Figures 4.5b and 4.5d) are drifting into the Boreas Basin. No pronounced drift pattern can be observed here.

Three more floats, 339, 341 and 342 (Figures 4.6a-c) are also drifting in the Greenland Basin, deployed during October 2005. They have been drifting too short to be able to distinguish any clear drift pattern. All the floats in the Greenland Sea are drifting at 1000m depths, except float 342, which is drifting at 1500m depths.

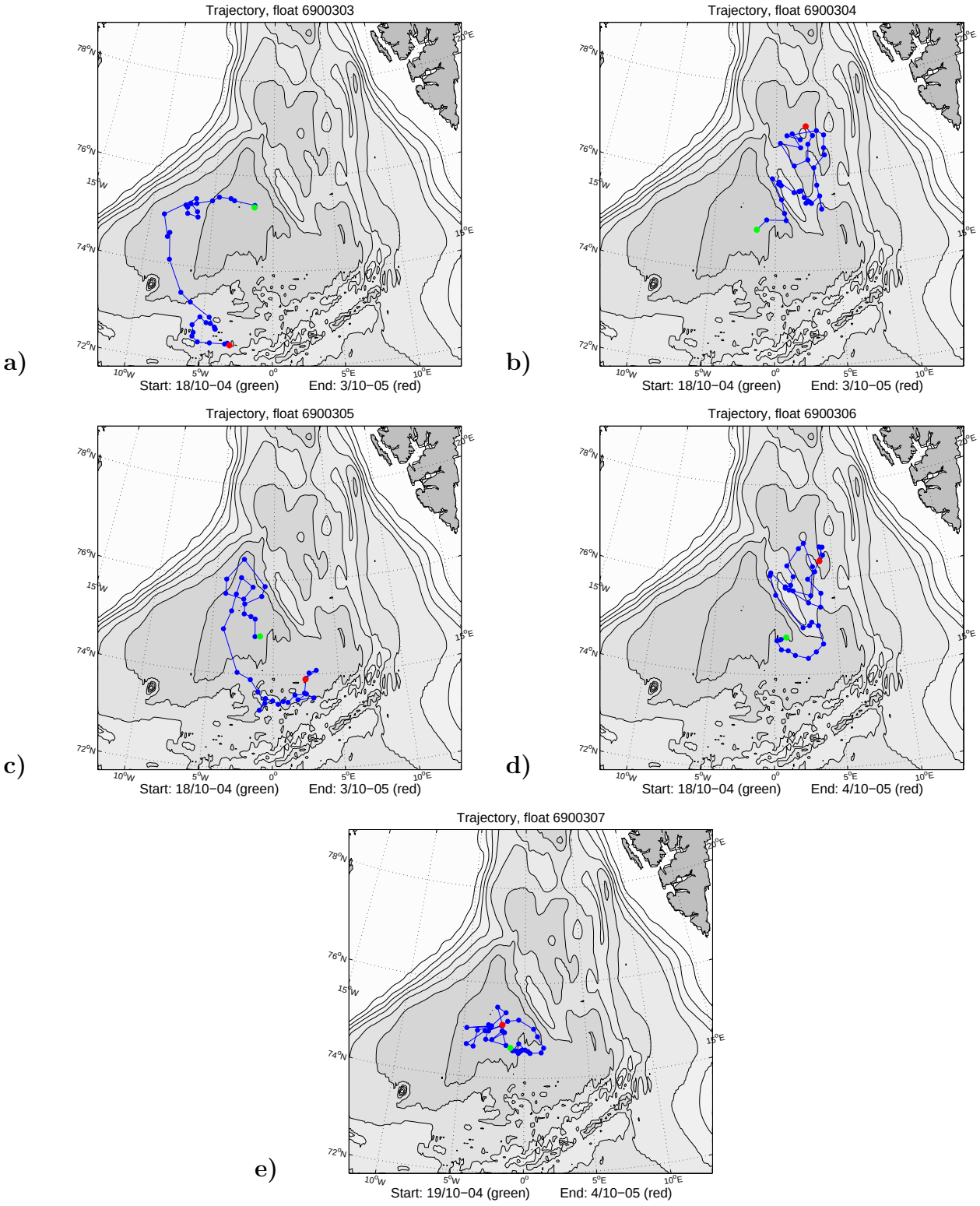

Figure 4.5: ***Trajectories of Argo floats deployed in the Greenland Sea during October -04. Parking depth is 1000m. a) Float 303 b) Float 304 c) Float 305 d) Float 306 e) Float 307.***

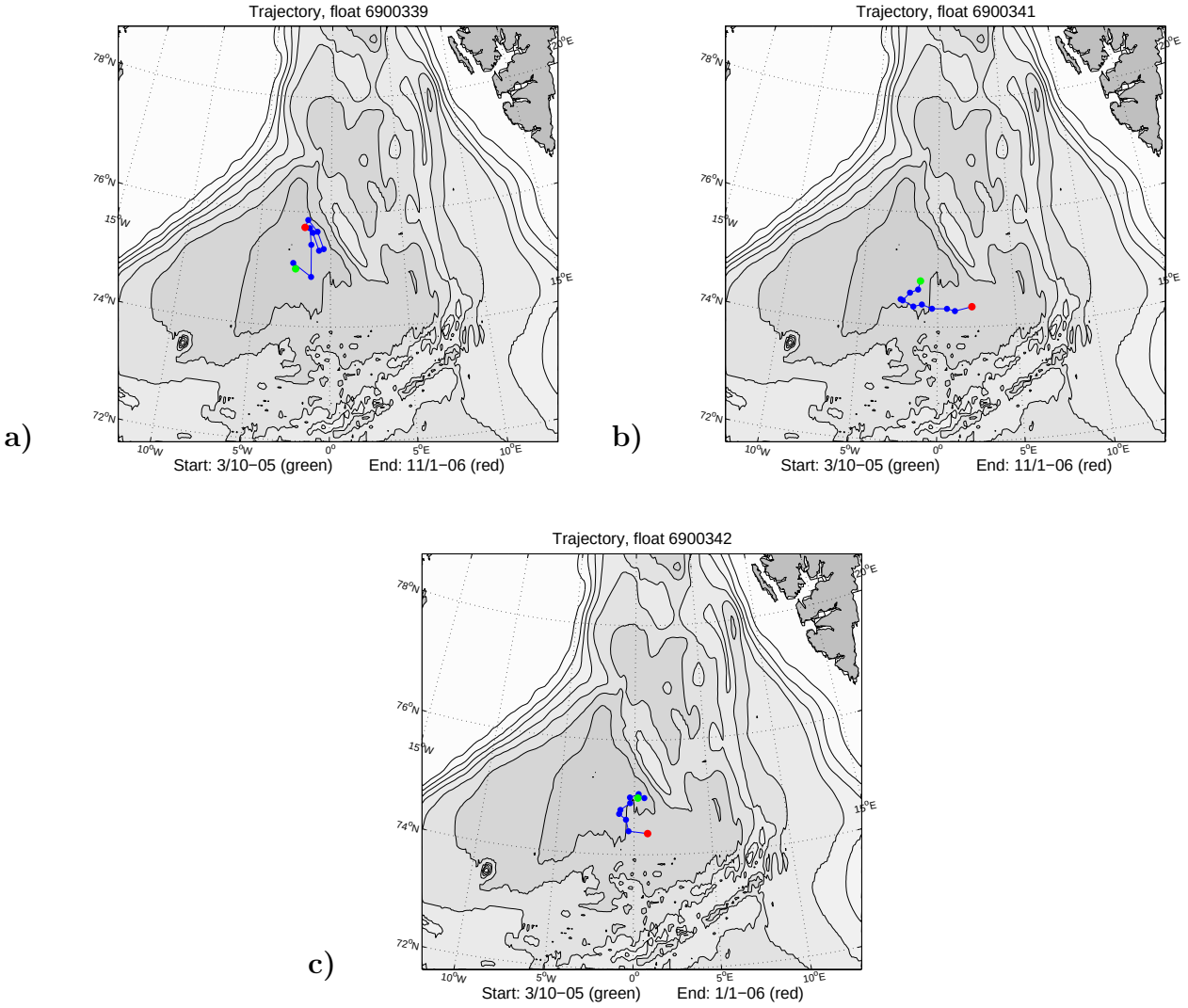

Figure 4.6: ***Trajectories of Argo floats deployed in the Greenland Sea during October -05: a) Float 339, parking depth is 1000m***
b) Float 341, parking depth is 1000m c) Float 342, parking depth is 1500m.

ICELAND SEA

There are three German floats in the Iceland Sea, 343-345 (Figures 4.7a-c). They have been drifting at 1000m depths for a few months only, and hence it is difficult to say much about the circulation pattern in the area, although it might be seen a tendency of cyclonic circulation. It is most pronounced for float 343 (Figure 4.7a).

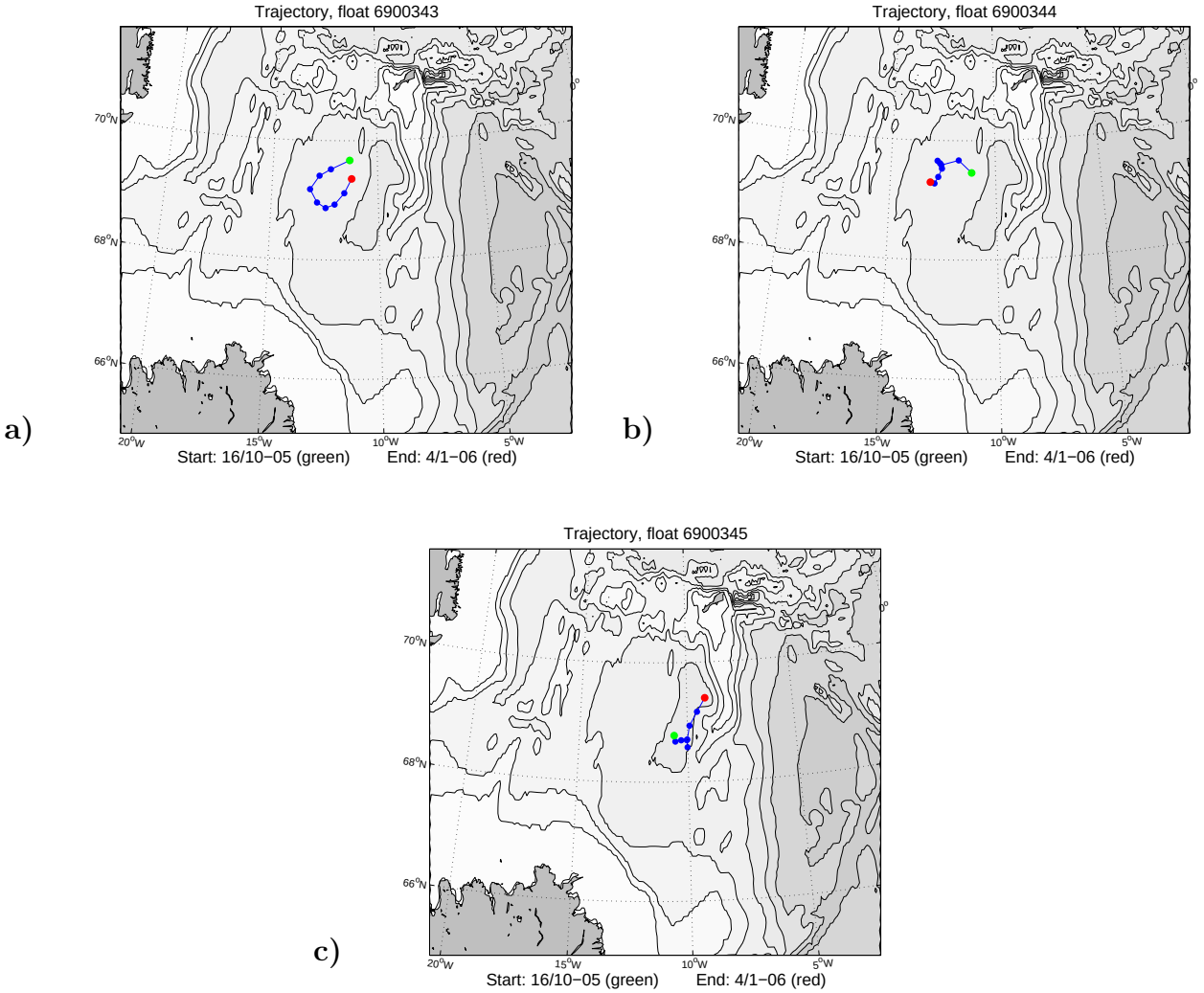

Figure 4.7: ***Trajectories of Argo floats deployed in the Iceland Sea, with parking depth at 1000m: a) Float 343 b) Float 344 c) Float 345.***

4.1.2 Temperature and salinity profiles

The Argo floats provide extensive information on the physical properties of the water where they are drifting. A gathering of profiles from the whole drifting period within each basin is used for presentation of temperature and salinity within the Nordic Seas. The drifting period for the Norwegian Basin, Lofoten Basin and the Greenland Sea cover at least one year, hence the following figures contain data from different seasons. The Argo temperatures are "in situ", not potential temperatures, and the water masses that will be referred to are those of table 2.1, defined by Blindheim & Østerhus (2005). Note that the different basins have different profiling depths.

Norwegian Basin
Figures 4.8a and b show typical temperature and salinity profiles for the Norwegian Basin. All the profiles obtained by float 216 are chosen as the representatives of the Norwegian Basin.

Generally in the Norwegian Basin, the temperatures are in the range of 4-14 °C at the surface layer and there is a sloping thermocline between 200-600m depths (Figure 4.8a). A more narrow range of temperatures can clearly be seen as one goes deeper. From 750m and down to 1300m depths all temperature measurements are between 0 and -0.8 °C. Evidence of a near homogeneously mixed upper layer is depicted for some of the profiles. This is due to a deepening in the mixed surface layer during wintertime.

Figure 4.8b shows the salinities, which at the surface are between 34.8 and 35.2. Both the temperature and salinity profiles clearly display the seasonal signal in the surface layers. The maximum salinities are found at depths around 100m, in waters that have originated from the Norwegian Atlantic Current (Blindheim & Østerhus 2005). Down to 600m depths there is a decrease in salinity. Between 500-950m depths many of the profiles have a salinity minimum of 34.89. This layer, underlying the Atlantic Water, is known as the Norwegian Sea Arctic Intermediate Water (NSAIW). Below 950m depths the salinities are more or less constant at about 34.90-34.91, which corresponds to the Norwegian Sea Deep Water (NSDW).

Lofoten Basin
The typical temperature and salinity profiles for the Lofoten Basin are shown in Figures 4.9a and b respectively. All the temperature and salinity profiles of float 218 are chosen as representatives of the Lofoten Basin.

The Lofoten Basin has temperatures between 4-14 °C at the surface as well (Figure 4.9a). There are more and deeper nearly vertical profiles in the upper layers com-

pared to the Norwegian Basin. Also the thermocline is deeper, located at depths of 600±200m. It is rather strong with temperatures rapidly decreasing from about 6 °C to 0 °C. From the depths of 1000m to 1300m nearly all temperature measurements are between 0 and −0.8 °C.

Compared to the Norwegian Basin, the salinity of the Lofoten Basin has a slightly larger range at the surface, but the maximum salinities is also located at 100-200m depths. Between 300 and 600m depths it is saltier than the Norwegian Basin. Decrease in salinity occurs down to 900m depths where it stabilizes at about 34.9 all the way down to 1300m depths. The intermediate water observed in the Norwegian Basin is also present in the Lofoten Basin, identified with salinities less than 34.9 and temperatures between −0.5 and 0.5 °C. Although not that pronounced, it is found between 600-1100m depths and hence located at greater depths than it was further south. The Lofoten Basin has a deeper and clearer halocline than the Norwegian Basin, and together with the thermocline it marks the bottom of the inflowing Atlantic Water, which occupies the upper 500-800m.

Greenland Sea

For the Greenland Sea, that means both the Greenland Basin and the Boreas Basin, the typical profiles are shown in Figure 4.10. There are some small differences between those two basins that will be pointed out in the description of the figures. Profiles obtained by float 305, which is drifting in the Greenland Basin, are the representatives for these two basins.

The Greenland Sea is colder at the surface, compared to the two previous basins, with temperatures ranging from −1 °C to 7 °C (Figure 4.10a). A thermocline is situated at about 100m depths for most of the profiles, and between 400-2000m depths the temperatures are approximately constant and slightly above −1 °C. Between the two basins in the Greenland Sea, the Boreas Basin has some higher temperatures than the Greenland Basin in the upper layers. This cannot be seen on this figure, as it only shows profiles obtained in the Greenland Basin.

The surface salinity gives the largest difference between the two basins in the Greenland Sea, as it in the Greenland Basin ranges between 34.4-34.9 approximately while it is between 34.4 and 35.1 in the Boreas Basin. The salinity in the Greenland Sea never exceeds 35.0. In both basins the salinity is approximately constant at about 34.9 between 400-2000m depths. All in all the profiles of both basins have similar behaviour. The Greenland Sea contains substantial amounts of Arctic Waters, and the deep waters originating from the Arctic Ocean can be identified as the salinity maximum of 34.91 at 1500-2000m depths

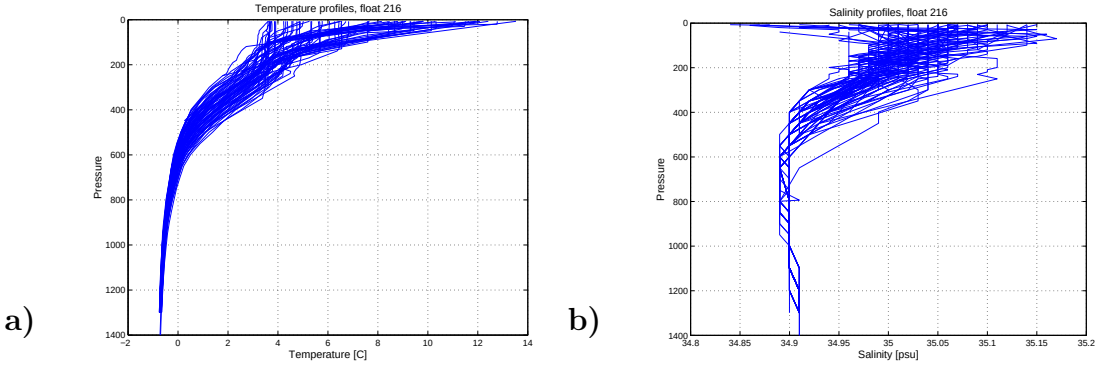

Figure 4.8: ***All a) temperature profiles and b) all salinity profiles of float 216, representing the Norwegian Basin.***

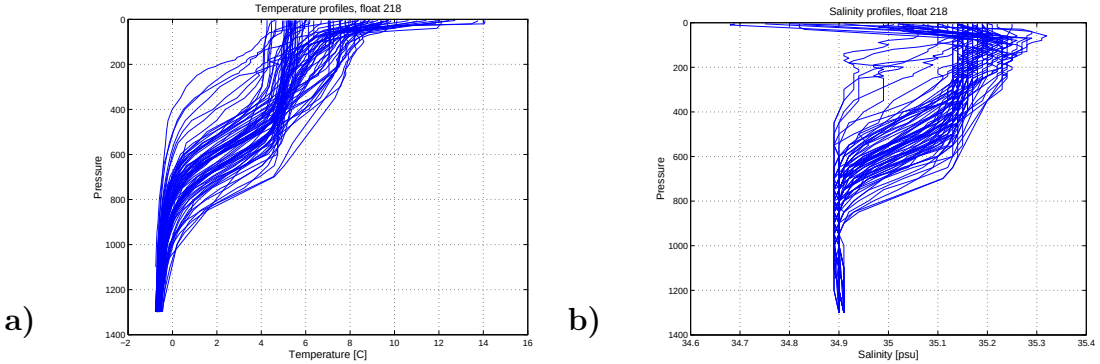

Figure 4.9: ***All a) temperature profiles and b) all salinity profiles of float 218, representing the Lofoten Basin.***

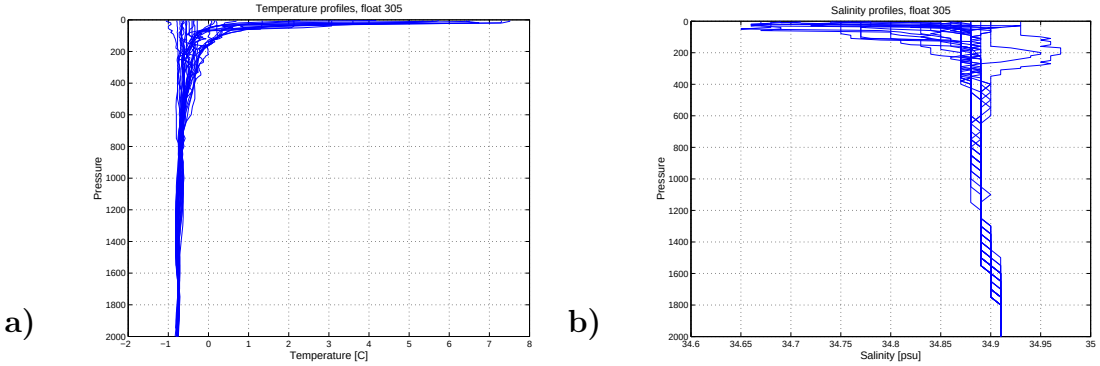

Figure 4.10: ***All a) temperature profiles and b) all salinity profiles of float 305, representing the Greenland Sea.***

Iceland Sea

For the Iceland Sea there are few data, but the typical temperature and salinity profiles for this area, represented by float 345, are shown in Figures 4.11a and b.

a)

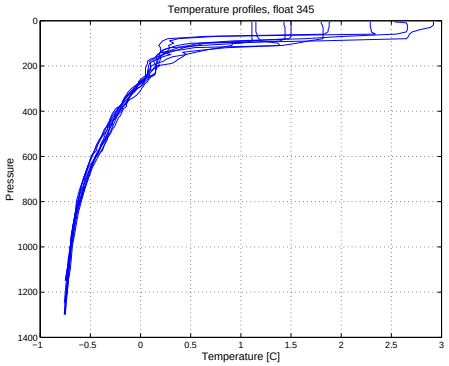

b)

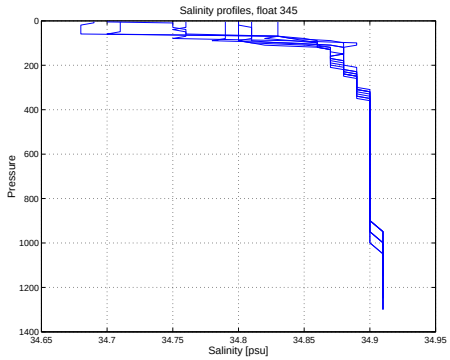

Figure 4.11: ***All a) temperature profiles and b) all salinity profiles of float 345, representing the Iceland Sea.***

In the Iceland Sea the temperatures are between 1-3 °C at the surface (Figure 4.11a), according to the few measurements from this data set. The data are obtained during some few months, from mid of October '05 to the beginning of January '06. There is a thermocline at about 100m depths. From 100m and down to 1300m depths the temperatures decrease gradually, from about 0.5 to -0.75 °C. The salinity is around 34.7-34.8 in the surface layer and increases to 34.9 at depths. The deepest measurements have salinities of 34.91 and are referred to as the Iceland Sea Deep Water.

4.2 Comparison Argo - Mike

This study directs no attention on validation of the Argo data itself. Although the data have passed through several quality checks, it is of interest to compare Argo data against other in situ data for further validation. Only a small test is done here, with data from the Ocean Weather Station Mike (Station M) chosen for this purpose. It is situated at 66 °N, 2 °E in the Norwegian Sea. Standard meteorological routines and hydrological observations have been made here since 1948. The oceanographic observation program is daily Nansen casts with a deep station once every week. For an open ocean water column, this is one of the longest and most complete time series there is (Gammelsrød et al. 1992).

The Argo profile that was taken closest to the position of Mike (66 °N, 2 °E) was found at 65.87 °N, 1.59 °E and obtained at the 19^{th} of February 2004. The profile obtained at Mike is taken the 18^{th} of February 2004. It is assumed that the water column doesn't change much during one day, at least not in the deep water. The temperature and salinity profiles are seen in Figures 4.12a and b respectively.

a)

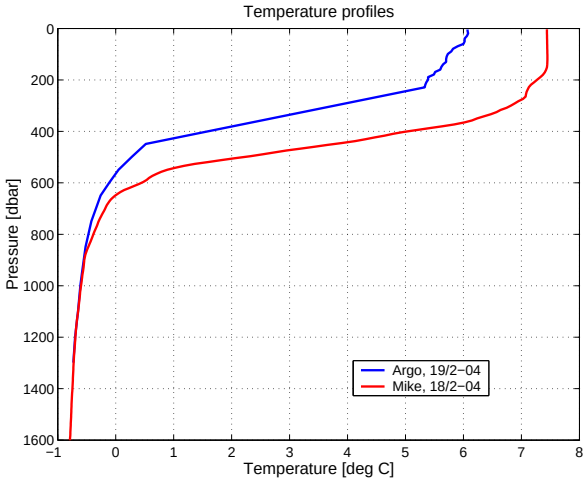

b)

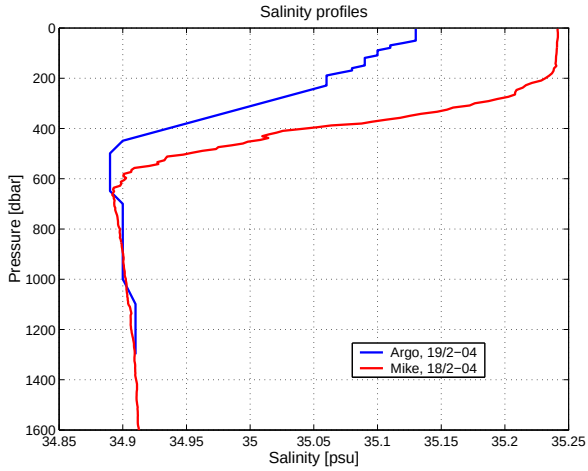

Figure 4.12: ***Comparison of temperature (a) and salinity profiles (b) obtained by Argo (blue) and Mike (red).***

From the depth of about 700m and deeper, the temperature and salinity profiles are approximately equal for both measurements. In the upper layer the temperature at Mike is in general a few degrees warmer than what is measured by the Argo float. The salinity is also higher, about 0.1 more at Mike compared to Argo. The time deviation on this scale is most probably not the reason for the deviation in the physical properties. If the instruments were incorrect calibrated, the differences would have been seen throughout the whole water column. As both Argo and Mike have the same values

below 700m depths, we can assume that the data are good. This region is a frontal area with large horizontal gradients in the east-west direction; see Figure 4.13a and b with temperature and salinity sections along 66 °N (Gammelsrød & Holm 1984). The Argo profile is taken a bit southwest of Mike, so a possible explanation can be that Mike is lying more into the North Atlantic Drift and hence has warmer temperature and higher salinity in the upper layers.

The distance between the positions of the two profiles is not more than 20km. It is striking how large the differences in temperatures and salinities are for the upper layers. This is the state in frontal regions. There are large variations in physical properties of the water over relatively short horizontal distances. When it comes to modelling, this is an issue. To get really good results, the model resolution must not be too coarse.

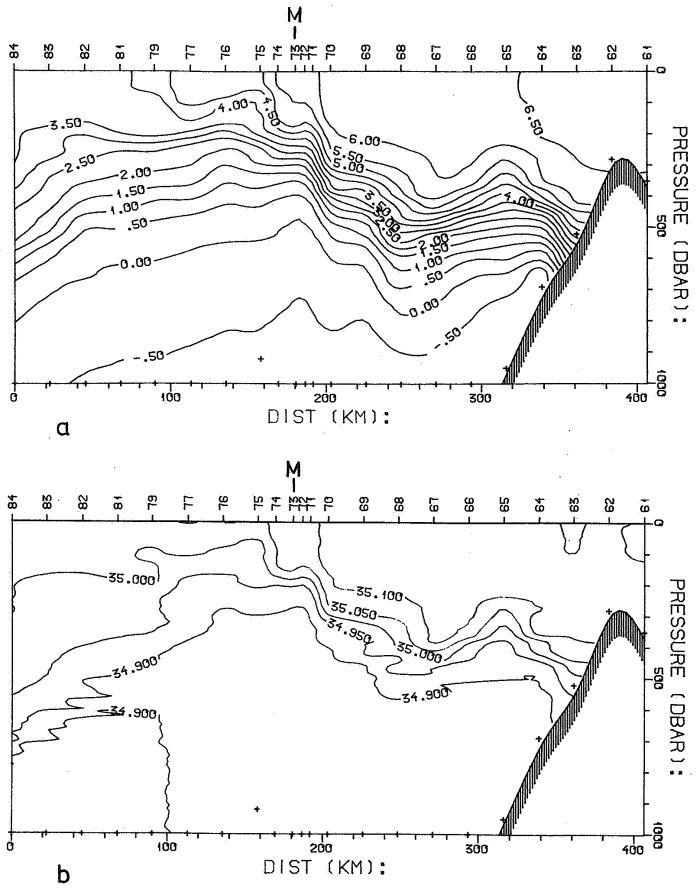

Figure 4.13: ***Section of (a) temperature and (b) salinity along*** 66 °N ***obtained in March 1983. M indicate the position of Mike. Figure is taken from Gammelsrød & Holm (1984).***

4.3 Deep-water currents obtained by Argo

There have been rather few observations of the deep ocean circulation in the Nordic Seas until the Argo floats were deployed. Figure 4.14 gives an overview of the velocities calculated from all the floats in the Nordic Seas. Red arrows are shown for velocities larger than 10 cm/s while the blue ones are for velocities less than 10 cm/s.

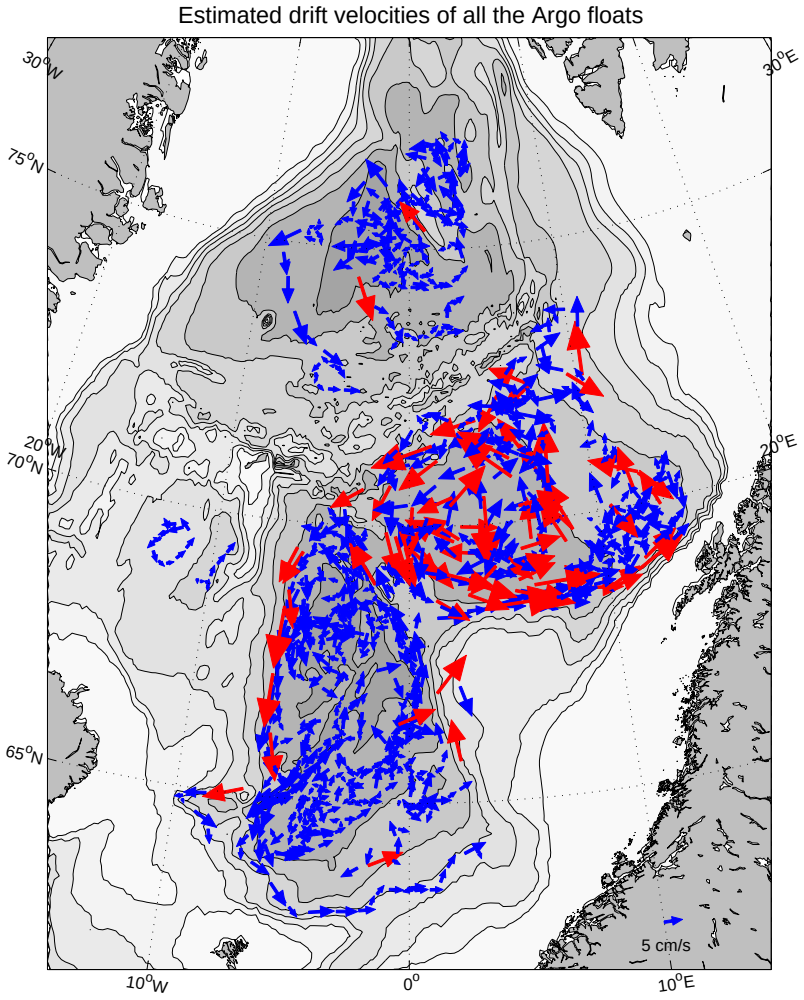

Figure 4.14: ***Deep water (1000 and 1500m depths) velocities obtained by Argo floats. Red arrows show velocities larger than 10 cm/s, blue arrows show velocities less than 10 cm/s. In the lower right corner there is a reference arrow of 5 cm/s and isobaths are drawn every 500m. Updated from Mork & Søiland (2006).***

We assume that the drift of the Argo floats corresponds to the deep water circulation. In general a cyclonic circulation is seen in all basins. The Iceland Sea (IS) does not have much data, but there is still a tendency of cyclonic circulation here. In the basins of

the Norwegian Sea this pattern is seen quite clear, especially at the outer parts. In the middle of the basins the drift seems a bit more complex. The current vectors indicate a rather strong topographic steering as it looks like most of them are oriented along the isobaths. In the Greenland Sea (GS) the topographic steering doesn't look that pronounced, but most of the drift nevertheless takes place above relatively flat areas. The flat area in the middle of the Lofoten Basin (LB) shows the same occurrence. The floats seem to drift more randomly in the absence of steep slopes. The topographic steering will be further examined in section 5.1.

Table 4.1 gives an overview of the estimated velocities of each Argo float. The mean velocity, standard deviation, maximum velocity and length of record are presented. Notice that there are large differences in the length of record and hence in the amount of data that forms the basis for calculation of the mean velocities. The Norwegian Basin (NB) has the longest time series, followed by the LB, the GS and at last the IS, which only has 3 months of records. The floats with largest mean and maximum velocities are found in the LB.

Table 4.2 shows the total mean velocity and standard deviation of each of the four main regions, while Figure 4.15 gives a sketch of the seasonal variations here. Due to the differences in length of records, some of the monthly means contain data from several years, while others are the mean of one month during only one year. E.g. for the NB, the November mean velocity is calculated from November 2002, November 2003, November 2004 and November 2005 while for the IS, it is calculated from data obtained during November 2005 only. This can influence and disturb the given results, but still the figure gives an indication of the velocity variations in the different regions.

The LB obviously has the largest current velocities (Figure 4.15). Throughout the year, the mean velocity here is always larger than in any of the other regions. This is confirmed by Table 4.2, which states that the total mean for the LB is about twice as large as for the NB, GS and IS. Figure 4.15 shows that the LB has largest velocities during the first half of the year, with a maximum peak in February. During the second half of the year, the monthly mean velocities are always less than the total mean for this basin, with a minimum in November. The LB also has the largest standard deviation (Table 4.2), indicating the largest seasonal variations. The NB has its maximum velocities in May. Throughout the rest of the year the monthly means do not vary much. The GS has its maximum peak in April, while the smallest velocities are found during September to December. There are larger variations in the monthly means for the GS compared to the NB, while the total mean velocities are approximately the same for these two regions. Even though Figure 4.15 indicate a larger seasonal velocity variation in the GS than in the NB, the total STD (Table 4.2) is slightly larger for

Name	Mean velocity [cm/s]	STD [cm/s]	Max velocity [cm/s]	Length of record [number of months]	Drifting area
6900215	3.4	2.0	9.7	40	NB
6900216	2.9	1.9	9.3	40	NB
6900217	3.9	1.9	9.2	34	NB
6900218	6.5	3.6	15.9	27	LB
6900219	5.4	3.5	17.3	27	LB
6900220	5.5	3.6	17.8	26	LB
6900221	4.3	3.2	17.0	26	NB
6900222	3.1	2.2	13.8	27	NB
6900223	5.0	4.2	19.4	26	NB/LB
6900303	3.0	2.4	9.6	12	GS
6900304	3.3	2.0	8.1	12	GS
6900305	3.8	2.3	12.4	12	GS
6900306	3.6	2.4	10.5	12	GS
6900307	3.2	1.9	7.1	12	GS
6900328	8.5	3.6	14.4	7	LB
6900329	7.2	5.0	19.8	7	LB
6900330	6.3	4.2	16.6	7	LB
6900331	5.2	2.6	9.9	7	LB
6900334	4.7	3.2	13.0	7	NB
6900335	2.2	0.9	3.7	7	NB
6900336	3.0	2.5	11.4	7	NB
6900339	3.3	2.0	7.2	3	GS
6900340	3.5	1.7	6.4	3	NB
6900341	2.4	1.0	3.9	3	GS
6900342	2.1	1.0	4.3	3	GS
6900343	3.1	0.8	4.5	3	IS
6900344	1.9	1.3	3.9	3	IS
6900345	2.1	1.0	3.5	3	IS

Table 4.1: ***Estimated mean and maximum velocities, STD and drifting time of each Argo float in the Nordic Seas (NB=Norwegian Basin, LB=Lofoten Basin, GS=Greenland Sea, IS=Iceland Sea).***

the NB than for the GS. The reason is that there must be larger velocity variations within each month for the NB. Recall that the floats in the GS have been drifting for maximum one year, while some of the floats in the NB have been drifting for about three and a half year. A longer data set will give larger variations, as the Argo floats are not in the same areas from one month the first year to the same month the next year. There can be different areas within the basin that have typical larger or smaller

	Mean velocity [cm/s]	STD [cm/s]
Norwegian Basin	3.4	2.3
Lofoten Basin	6.3	3.9
Greenland Sea	3.3	2.1
Iceland Sea	2.4	1.1

Table 4.2: ***Mean velocities and STD of the basins in the Nordic Seas.***

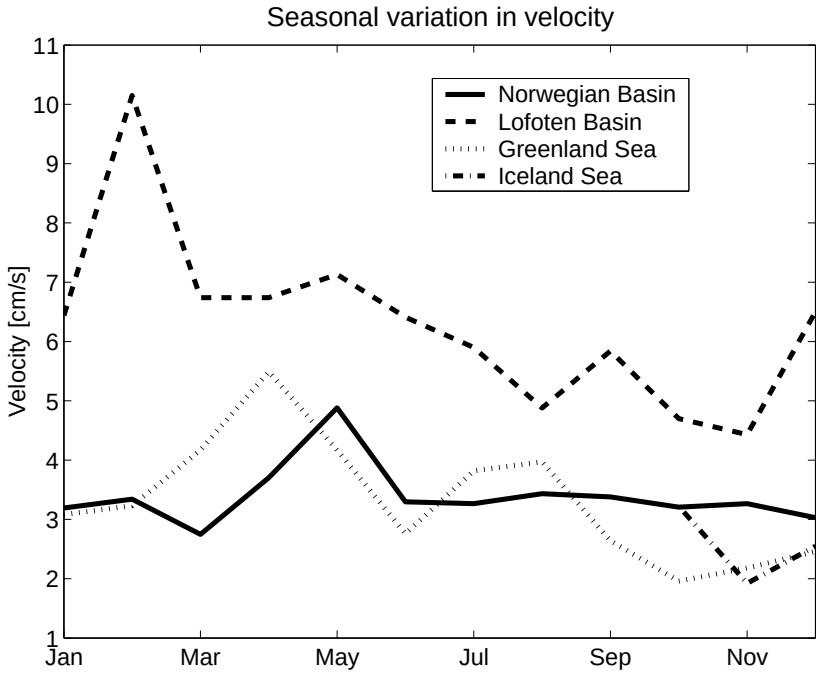

Figure 4.15: ***Monthly mean velocities for the Norwegian Basin, the Lofoten Basin, the Greenland Sea and the Iceland Sea. Updated from Mork & Søiland (2006).***

velocities independent of the time of the year. Hence it is not necessary the reality that there are larger seasonal variations in the GS than in the NB. The LB and NB have however about the same length of records. The STD of the LB is 1.6 cm/s larger than the STD of the NB, which do imply stronger seasonal variations in the LB than in the NB. The IS has the smallest total mean velocity and STD. The data are obtained during the three last months of the year, the time where the other regions generally have their smallest velocities. Due to the sparse data, no further interpretation of this region is possible.

4.4 TS-diagram

To present the watermasses in the Nordic Seas, a TS-diagram (Figure 4.16) is made. The blue dots are Argo data while the red ones are data from the TOPAZ model. All Argo floats within the Nordic Seas are considered, but due to the restrictions of the model data, only profiles obtained during January-September 2005 are extracted. The model data are interpolated to the observed profiles. Density curves (σt) are added to the diagram and the definition of the major watermasses in the Nordic Seas are indicated (see the caption of Figure 4.16).

An obvious feature is that the modeled water masses and the water masses measured by Argo have distinct locations in the TS-diagram. The main part of the Argo watermasses have densities larger than $\sigma t = 27.7$, while the modelled water masses mainly have densities below $\sigma t = 27.7$. For the deepest water masses, which have low temperature and salinity, the model data are in general saltier than the Argo data. This is most likely due to a known exaggerated mixing in the model, south of Greenland. This leads to an overestimation of temperature and salinity in the deep waters here. Notice that the NSAIW is only covered by the Argo data. Some of the watermasses have rather few or no measurements that fit within the definitions. This is because the amount of measurements is restricted, and during this time period the Argo floats may not have been in all areas where the different watermasses are located.

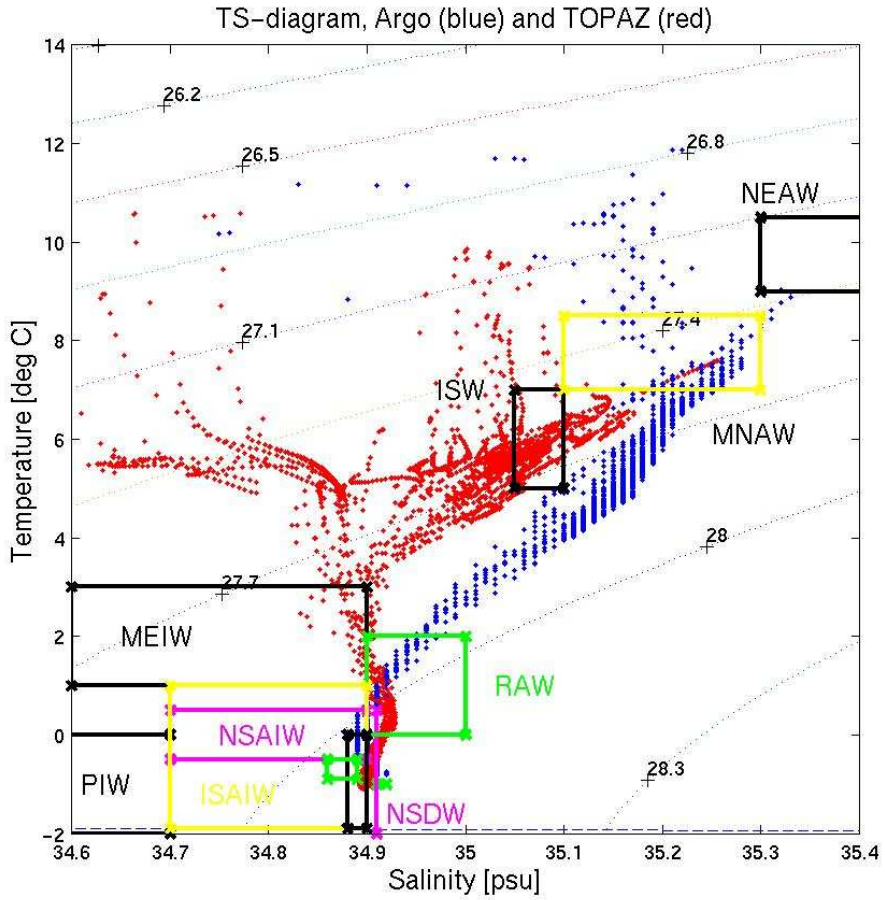

Figure 4.16: ***TS-diagram for the Nordic Seas, blue dots are Argo data, red dots are Topaz data. The indicated water masses, starting from the top, are:***
North East Atlantic Water (NEAW - black), Modified North Atlantic Water (MNAW - yellow), Irminger Sea Water (ISW - black), Modified East Icelandic Water (MEIW - black), Recirculating Atlantic Water (RAW - green), Iceland Sea Arctic Intermediate Water (ISAIW - yellow), Norwegian Sea Arctic Intermediate Water (NSAIW - magenta), Norwegian Sea Deep Water (NSDW - magenta), Greenland Sea Deep Water (GSDW - black), Polar Intermediate Water (PIW - black), Greenland Sea Arctic Intermediate Water (GSAIW - green) and Iceland Sea Deep Water (ISDW - green). Definitions by Blindheim and Østerhus (2005), see Table 2.1.

Chapter 5

Discussion

5.1 Topographic steering

The interpretation of the previous trajectory figures (Figures 4.1 - 4.7) and the current vector plot in Figure 4.14 led to assumptions of rather strong topographic steering on the drift of the Argo floats. Especially floats 216 and 217 show a very pronounced topographic steering in the area 4-7 °W and 64-66 °N. A blow up of the trajectories of these floats within this area are shown in Figure 5.1. The red dots indicate the first pass of the Argo float, while the blue dots indicate the second pass. Although this figure leaves no doubt that the drift of the Argo floats are influenced by the bathymetry, this strong relation is not present throughout the Nordic Seas. For further examination of this phenomenon, the deviations from ideal topographic steering were computed. The

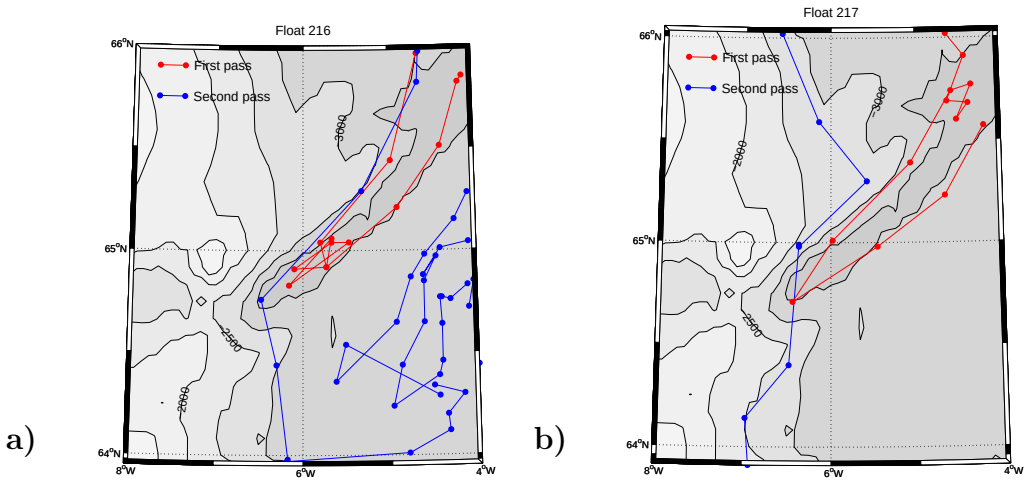

Figure 5.1: ***A blow up of the trajectories of Argo float 216 (a) and 217 (b). Red dots indicate the first pass, blue dots the second pass. Bottom contours are drawn every 500m (Idea from Mork & Søiland (2006)).***

coordinate system was rotated such that the x-axis was parallel to the isobaths, with larger depths above the x-axis, i.e. a cyclonic circulation around topographic lows. The angle θ is the angle between the new along-contour x-axis and the velocity vector. $\theta = 0\,^\circ$ for ideal topographic steering. $\theta = 90\,^\circ$ means that the current is perpendicular to the isobaths. $\theta = 180\,^\circ$ means that the current is parallel to the bottom contours, but with larger depths to the right. A profound description on the theory of topographic steering can be found in e.g. Gill (1982).

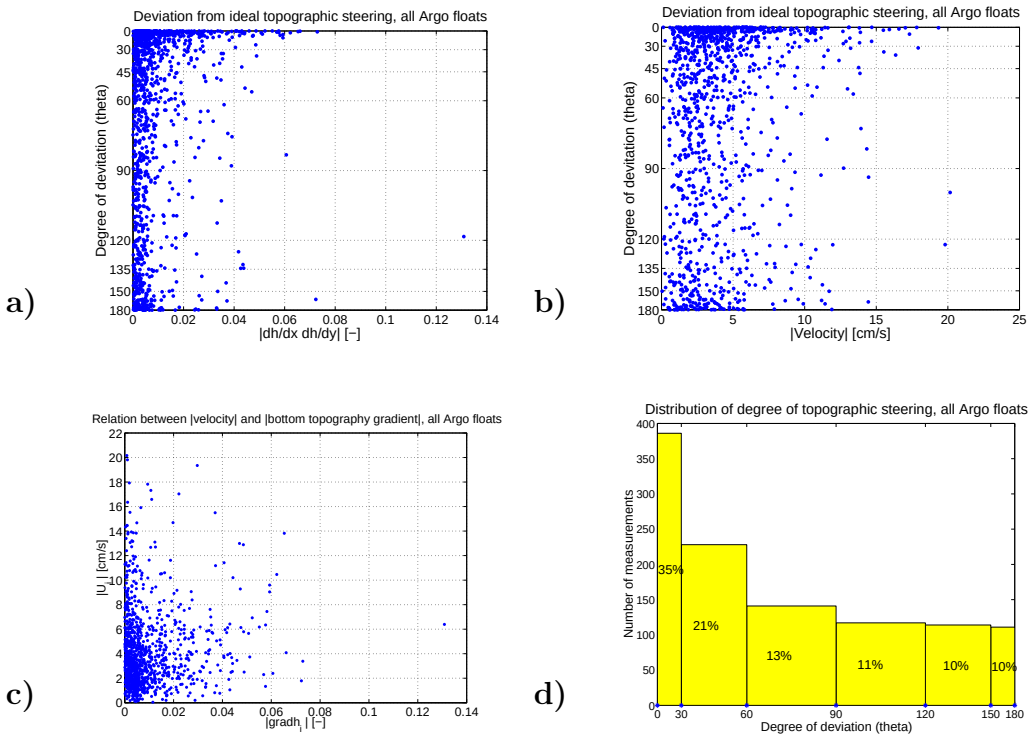

Figure 5.2: ***Degree of deviation from ideal topographic steering for all Argo floats to the length of the bottom topography gradient (a) and to the length of velocity (b). c) shows the length of velocity to the length of the bottom topography gradient. d) shows the distribution of degree of topographic steering for all Argo floats. See main text for further explanation.***

The assembly of all Argo floats in the Nordic Seas is first discussed. Figures 5.2a and b show the degree of deviation from ideal topographic steering to the length of the bottom gradient and to the length of the velocity respectively. The topography gradients are calculated at the points where velocity estimates exist. According to theory, larger topography gradients should lead to stronger topographic steering. There should also be a correlation between the steepness and the velocity, and hence larger velocities should correspond to stronger topographic steering as well. A tendency of stronger topographic steering as the steepness and velocity gets larger can be seen in Figures

5.2a and b respectively, but it is not significant. Figure 5.2c shows the relation between the length of the topography gradient and the velocity, but no correlation is seen.

Figure 5.2d shows the distribution of θ without taking the size of the steepness and velocity into consideration. Totally there are 1097 velocity estimates from all Argo floats within the Nordic Seas. 35% of all the velocity estimates deviate less than 30° from the along contour lines.

Flat areas will theoretically make the current drift more randomly and lead to larger θ. This was not significant according to Figures 5.2a and b. An attempt is done trying to discover whether there is a pattern of where the topographic steering is strong.

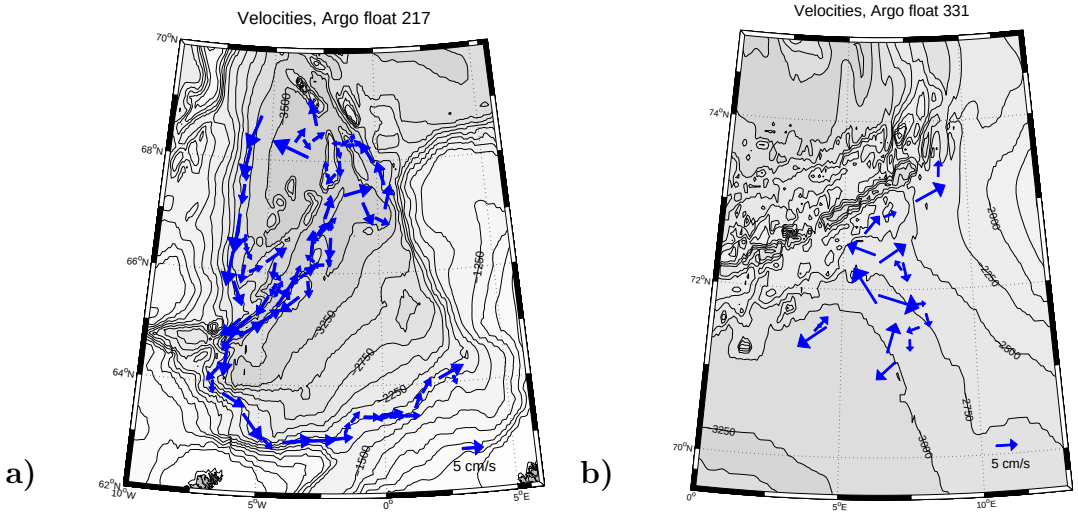

Figure 5.3: ***Current vectors of float 217 (a) and 331 (b).***

The current vectors of two single Argo floats, float 217 drifting in the Norwegian Basin and float 331 drifting just north of the Lofoten Basin, are shown in Figures 5.3a and b respectively. Visually the figures imply that float 217 is highly steered by the topography while float 331 is not. This is confirmed by Figures 5.4 and 5.5, showing the same calculations as in Figure 5.2, for each of the two floats. Float 217 has 94 velocity estimates while float 331 only has 19. Figures 5.4a and b shows that float 217 to a certain extent has larger topographic steering as the length of the topography gradient and velocity increases. There is still no correlation between the bottom steepness and the velocity, as seen in Figure 5.4c. Figure 5.4d shows that 57% of the velocity estimates have a deviation of less than 30° from the bottom contours. This is rather good. Float 331 does not have such good results. In Figures 5.5a and b no tendency of stronger topographic steering is seen at all as the length of the bottom topography gradient and the velocity increases.

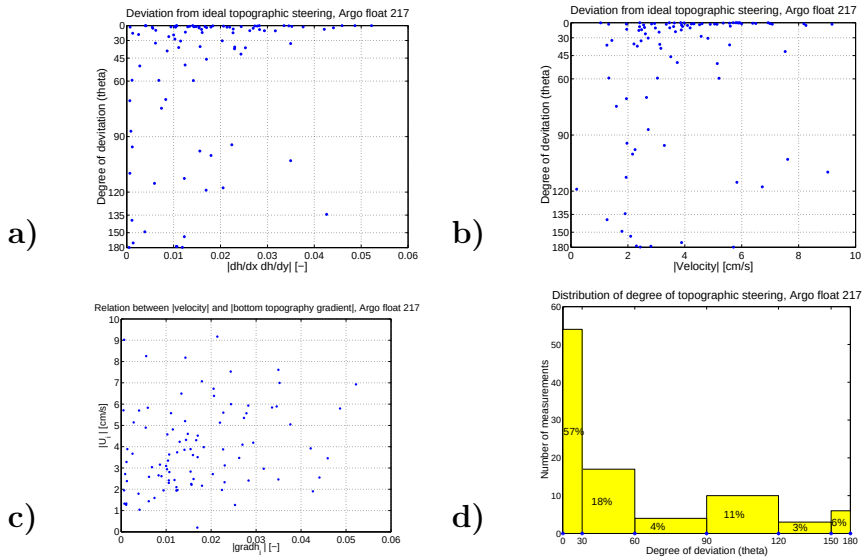

Figure 5.4: ***Same as figure 5.2, but only considering Argo float 217.***

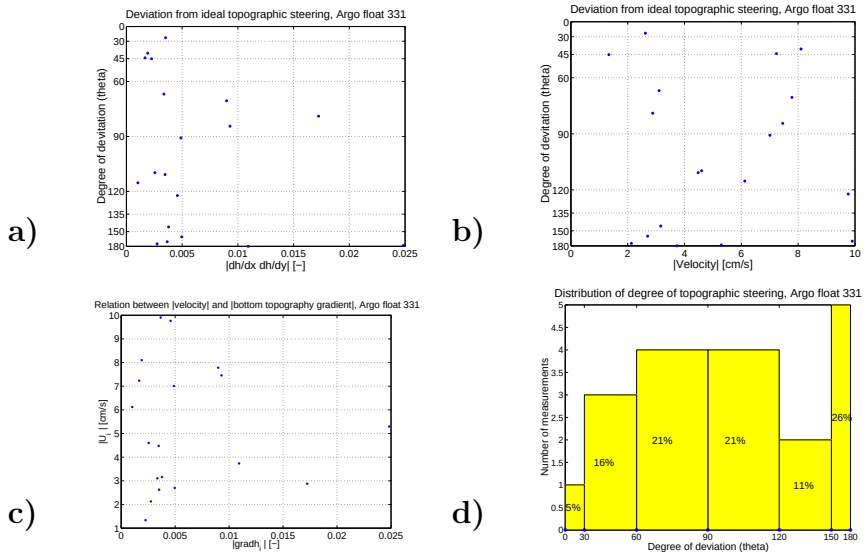

Figure 5.5: ***Same as figure 5.2, but only considering Argo float 331.***

Neither is there any correlation between the length of the topography gradient and the velocity (Figure 5.5c). Figure 5.5d shows that only 5% of the velocity estimates have $\theta < 30\,^\circ$. The largest part of the velocity estimates (26%) is actually found between 150-180 $^\circ$ of deviation, which means that the current is drifting with larger depths to the right. In the area north of the Lofoten Basin, with the Mohn Ridge, the bathymetry is very complex. It is probable that this is influencing the currents in the area, and

hence float 331 is not steered by the bottom topography the theoretical way.

There is a weakness by computing the bottom topography gradients only at the points where the velocity estimates were made. The water is not only influenced by the bottom at the point just below it, but it will feel the bathymetry within a certain range. The size of this range will depend on both the bottom topography and the properties of the water masses. Still we can assume that the topography gradients at a single point in most cases are representative for the area. Seven separate areas within the Norwegian Sea were nevertheless chosen to find out if the currents in areas with steep bottom are more influenced by topographic steering than the currents above more flat areas. The areas A-G are pointed out in Figure 5.6a. The mean bottom topography gradients were computed for each area and used instead of gradients at single points. θ for each velocity estimate were then calculated as previously described and the results are shown in Figure 5.6b. Area A, B and C have the smallest mean bottom topography gradients and the deviations are regularly distributed in all directions. This is confirmed by Figure 5.6c, where the percentages of estimates within given ranges of deviations are shown for each area. The degrees of deviation are divided in 6 groups of $30\,^\circ$ between $0\,^\circ$ and $180\,^\circ$. The total numbers of velocity estimates within each area are given in the legend. For area A, B and C the degree of deviations are relatively even distributed among all the 6 groups. From this we can conclude that the currents in these areas are not primarily steered by the bathymetry.

Area D, E, F and G have respectively increasing mean bottom topography gradients and hence we would expect respectively stronger topographic steering. But as seen in Figure 5.6b area G has the largest spread among these four areas. Recall from the trajectories in Figures 4.3b and c that it was observed some chaotic movements in this area. The reason might be due to the gentle sloping between 2500 and 3000m depths northeast in the Lofoten Basin. The current is flowing above a rather steep slope until the bottom flattens out, leading to a divergence of the current. River run-off, tides and internal waves might also influence the current particularly in this area. These are just assumptions, and the reason for the chaotic movements in this area are not fully understood. From Figures 5.6b and c it follows that currents in area E has the strongest topographic steering, where all velocity estimates deviate less than $30\,^\circ$ from the ideal topographic steering. Also the currents in area F are strongly steered by the topography. There are two velocity estimates that are in the wrong direction. The reason is probably not that the current turns in the opposite direction only at these two points. An uncertainty considering the current estimates obtained by the Argo floats is the surface drift of the floats. According to the trajectories that mainly are close connected to the isobaths, we can assume that the surface drift in general is small and we can ignore it. This is because of the relatively short time period the float spends at

the surface. Still, if the wind and surface currents are strong, the velocity estimates of that day will be more influenced and the surface drift will in some cases cause a source of error. This can be a possible explanation. The remaining area D has a fairly strong topographic steering, but also here there are some velocity estimates directed in the wrong direction. Although there exist velocity estimates that deviate from the ideal topographic steering, it is clear that areas with larger topography gradients are more steered by the topography.

The first look on the Argo trajectory figures and the velocity vector plots made us assume that there was a rather strong topographic steering of the currents at the depths where the Argo floats are drifting. Figure 5.2 weakened this assumption, as there were about 44% of the velocity estimates that deviated more than 60 ° from the ideal topographic steering. On the other hand, the selection of seven different areas with different typical bottom topography gradients confirmed that currents above relatively flat areas are drifting more randomly than those above steeper bottom. It is then clear that the currents at these depths to some extent are influenced by the bottom topography, but there are many exceptions and the currents must additionally be influenced by other factors. Svendsen et al. (1991) found that for a 2-layer geostrophic flow, the topographic steering would propagate throughout the layers and also influence the upper layer circulation. In reality there are non-linear terms and the current is not stationary so that the conditions for ideal topographic steering is not completely fulfilled. Tidal forcing and the atmosphere, with atmospheric pressure and winds are also influencing the currents. The properties of the water masses throughout the water column will determine the currents in the way that large horizontal differences will give rise to baroclinic currents. These factors will all influence the circulation additionally of the bottom topography, and hence lead to deviation from ideal topographic steering. Other possible sources of errors for the above calculations are as mentioned that we use the topography gradient at a given point, or that we use the mean gradient over a selected area. The latter will probably give more correct results as it considers larger areas surrounding the current, but the selection of areas is important to get trustful results. It is necessary to choose areas with approximately the same gradients to benefit from the use of mean values. Also if the area is too big, the typical topography gradient can be very different within it and hence it is not sure that the velocity estimates should be steered by the calculated mean gradient. Finally we have to take into account that these velocities are only estimates from the drift of the Argo floats, where positioning takes place only every tenth day. And as mentioned, there are probably some deviations from the real currents at the drifting depths as the floats are drifting with the surface currents while they are transmitting data at the surface and also in intermediate depths during profiling.

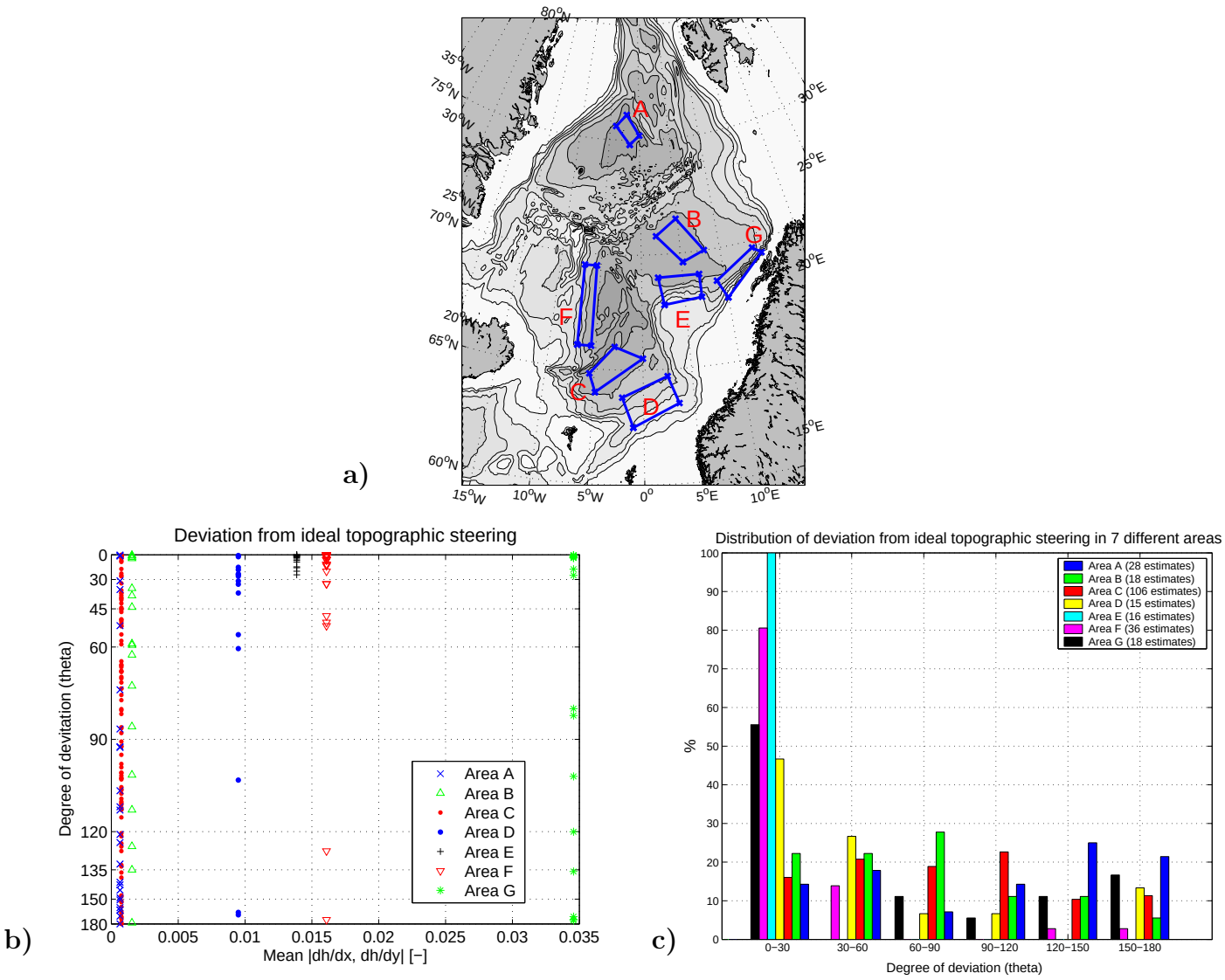

Figure 5.6: ***Selected areas, A-G, shown on the map in a), with different typical bottom topography gradients. b) The deviation from ideal topographic steering for all areas to the length of their mean bottom topography gradient. c) Distribution of the deviation for each area.***

5.2 Comparison of TOPAZ against climatology: Temperature and salinity

For investigation on how the TOPAZ model is doing, contour plots of temperature and salinity at selected depths were compared against the climatology. The monthly averaged GDEM (Teague et al. 1990) climatology is used, with a spatial resolution of $1/4\,^{\circ}$. For the model data, daily averages are used. In the Nordic Seas it has a spatial resolution of $1/3\,^{\circ}$. Model data from several days throughout a month were compared, and the differences were found small enough for a random day in the middle of the month to be used for comparison.

Contour plots of both temperature and salinity have been made for every month from January to September at 5 different depths; 0m, 50m, 200m, 700m and 1500m. Then difference plots were produced with climatology data extracted from the model data. The climatology is highly variable in the upper layers, so the comparisons here are not really useful. Only results from 200m and 1500m depths will be shown.

Figures 5.7 and 5.8 show modelled (a) and climatology (b) contour plots of temperature and salinity at 200m depths respectively. The differences among those two (TOPAZ-climatology) are shown in Figures 5.7c and 5.8c. The temperature difference scale is from $-5\,^{\circ}$C to $+5\,^{\circ}$C while the salinity difference scale is ranging from -0.5 to $+0.5$. Differences larger than these values are not shown in the figures. On this scale, there were small variations among the different months, and I will therefore only show the results from one month, April. The contour plots (Figures 5.7a-b and 5.8a-b) show that the inflow of modelled warm and saline Atlantic water are spread more into the middle of the Norwegian Basin than the climatology indicates. The climatology shows warm and saline water situated more along the Norwegian continental shelf break, with both temperature and salinity contours nearly parallel to the break. The modelled contours are much more complex, and near the Norwegian coast they are almost perpendicular to it. This is the most pronounced feature on the contour plots.

The difference plots (Figures 5.7c and 5.8c) show where the model overestimates and where it underestimates the values. TOPAZ is mainly warmer than climatology at 200m depths, as seen on Figure 5.7c. Only in the eastern and mostly northeastern part of the Nordic Seas, the temperatures of the climatology are higher than the modelled ones, with about $2\,^{\circ}$C as maximum differences close to Svalbard. Additionally there is a small area at $70\,^{\circ}$N north of Iceland where the modelled temperatures are underestimated by about $1\,^{\circ}$C in relation to the climatology. In the Norwegian and Greenland Basins the largest overestimations occur, with more than $5\,^{\circ}$C differences.

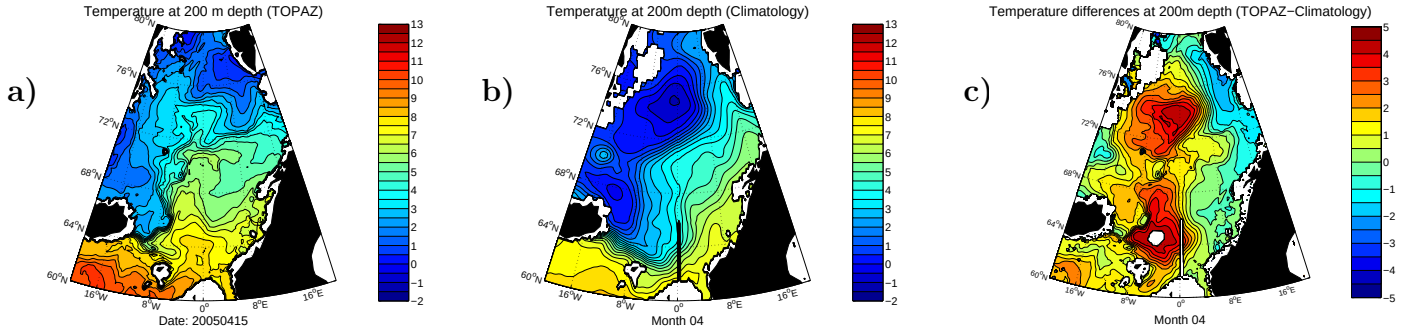

Figure 5.7: ***Temperatures at 200m depths (April) a) Modelled temperatures, TOPAZ b) Climatology c) Temperature differences between TOPAZ and the climatology***

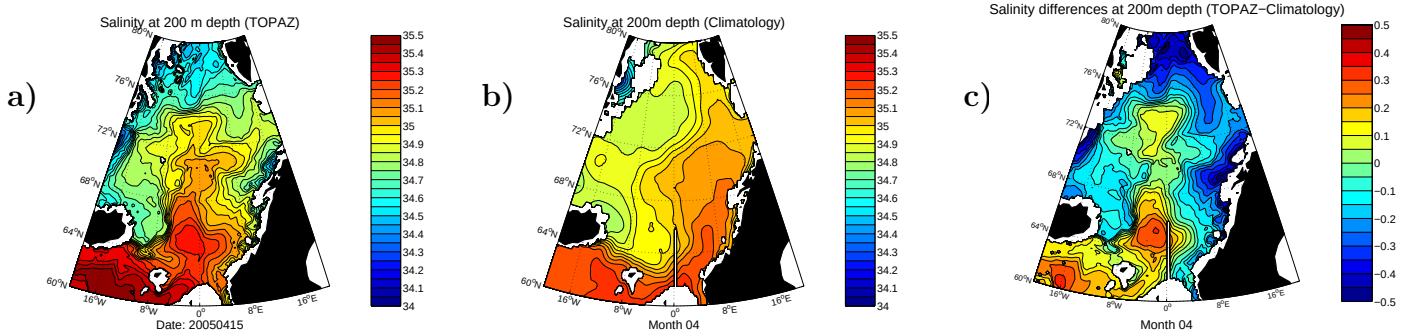

Figure 5.8: ***Salinities at 200m depths (April) a) Modelled salinities, TOPAZ b) Climatology c) Salinity differences between TOPAZ and the climatology***

In the same areas where the largest positive temperature deviations take place, overestimation of salinity occurs too, see Figure 5.7c. It is largest in the Norwegian Basin with maximum deviations of about 0.3. Overestimation of salinity in the Greenland Basin does not exceed 0.1. In the outer parts of the Nordic Seas, the modelled salinities are mainly too low compared to the climatology. The model is then saltier and warmer in the exterior of the NWAC and vice versa in the interior of the NWAC.

The results from 1500m depths are shown in Figures 5.9 and 5.10. The data are still from April. The difference scale for temperature is now ranging from $-1.5\,^{\circ}\mathrm{C}$ to $+1.5\,^{\circ}\mathrm{C}$, while for the salinity it is from -0.05 to $+0.05$. Again both temperature and salinity contours are more smooth for the climatology than for the model, see Figures 5.9a-b and 5.10a-b. The temperature differences (Figure 5.9c) show that the modelled temperatures are too high in the northern areas, but the deviation is not more than $0.6\,^{\circ}\mathrm{C}$. In the Norwegian Sea, the agreement between climatology and model is quite good, with largest deviation of $\pm 0.2\,^{\circ}\mathrm{C}$.

For the salinity (Figure 5.10c) there is also some overestimation to the north. Maximum deviation is not more than 0.015, and e.g. in the Boreas Basin there is a very good agreement between the climatology and the model. In the Norwegian Sea the modelled salinity is too low with 0.03 as maximum deviation, but in general the modelled salinity is not more than 0.015 lower than the climatology here.

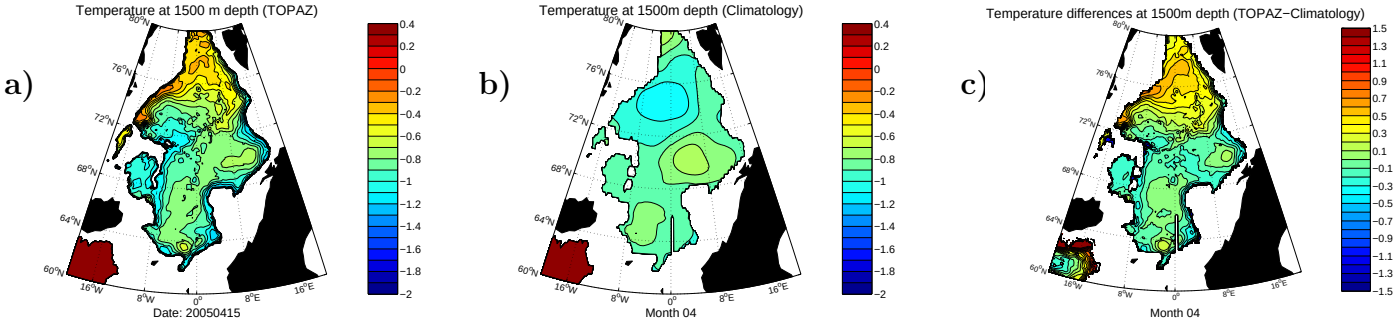

Figure 5.9: ***Temperatures at 1500m depths (April) a) Modelled temperatures, TOPAZ b) Climatology c) Temperature differences between TOPAZ and the climatology***

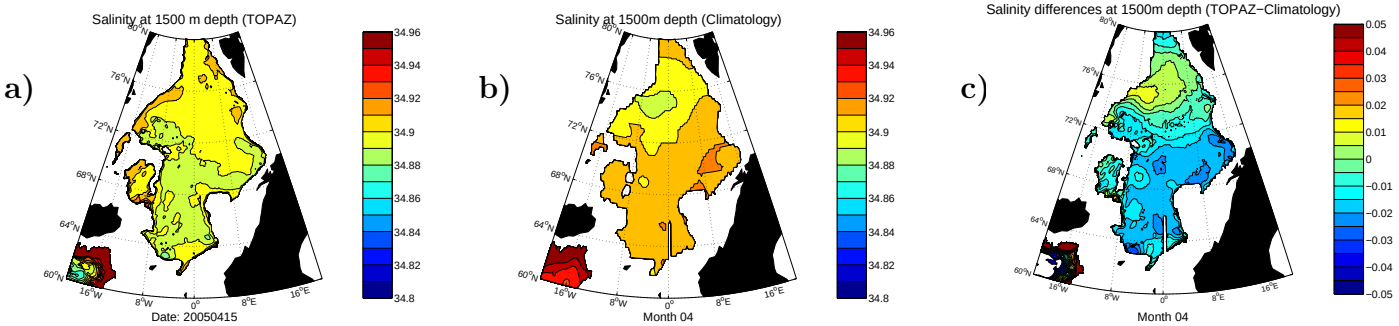

Figure 5.10: ***Salinities at 1500m depths (April) a) Modelled salinities, TOPAZ b) Climatology c) Salinity differences between TOPAZ and the climatology.***

This study shows that there is a closer agreement between TOPAZ and climatology at 1500m depths contrary to 200m depths. The model is initialized from climatology and additionally it assimilates SLA and SST as the model is running. At present there is no assimilation in the interior of the ocean. The model outputs at the surface are tied to the assimilated data while they at greater depths are influenced by the depth transformation of the assimilated surface data additionally of the model dynamics. Despite that the effect of assimilation is larger at 200m depths, the differences are larger here. At greater depths the water properties are more constant and hence easier to model.

5.3 Comparison Argo - Topaz: Temperature and salinity

The GDEM climatology only provides information about the rough structure of the ocean, but no details. It is not useful to check if a model describes seasonal phenomenon well. In situ data like Argo are on the other hand better for this purpose. An objective for the Topaz model is to have weekly updated comparisons against Argo on the Topaz validation page on Internet *(http://topaz.nersc.no/Class4)*. The data presentation should therefore be simple and user-friendly. One way to do this is to show maps with dots indicating differences between the model and the in situ data. For the Topaz model this is done weekly for the whole Atlantic Ocean, but in this thesis I will only focus on the measurements and comparison done in the Nordic Seas. Due to the contents of this data set and a change in the format of the model files, the time period is restricted from February to September 2005. All Argo profiles obtained during this period are used and compared against daily average data from the model.

In Figures 5.11 and 5.12 four different depth layers are made to visualize differences between Topaz and Argo throughout the water column. They are ranging from 0-50m (layer 1), 50-200m (layer 2), 200-700m (layer 3) and 700-1500m (layer 4). Both temperature and salinity maps are produced of the area 15 °W to 15 °E and 61-79 °N for each layer. For every profile, the differences between the model and Argo data are calculated at every depth where measurements are taken, and then the average difference for each layer is calculated. There are colored dots for every profile, indicating these average differences. The color scale is -3 to $+3$ °C for temperature and -0.5 to $+0.5$ for salinity. Values less/larger than this are set to the minimum and maximum values respectively. For this purpose we assume that the Argo data is the real values.

Originally these maps were made every week. When it comes to the Nordic Seas, some weeks contain almost no data while other weeks have up to 20 profiles taken. This makes it quite difficult to draw any conclusions. Data from the whole period are therefore gathered in one figure. Figures were also made for different months to see if the model is doing better or worse throughout the year. The data set was divided in three periods for this purpose, February to April, May to June and July to September. Those figures are not shown.

Figure 5.11 shows the average salinity differences (model - Argo). The deepest layer (Figure 5.11d) has definitely the best agreement. The differences between the model and the Argo data are close to zero for the whole Nordic Seas. To the north in the Norwegian Basin there is underestimation of salinity, with approximately the same magnitude in all the three upper layers. Modelled salinities here are maximum 0.2 to

low. South in the Norwegian Basin the modelled salinities are in general too high, with maximum deviation of 0.3. The largest overestimation takes place between 200-700m depths (Figure 5.11c), but also in layer 2 (Figure 5.11b), the salinity differences are larger than in the upper layer (Figure 5.11a).

There are more similarities among the three upper layers in the Lofoten Basin. Modelled salinities are too low here, with the largest deviations to the east. In layer 1 and 2 the underestimation has a maximum of -0.5 close to the north Norwegian coast. Layer 3 is slightly better, with salinities maximum 0.4 too low.

Along and slightly to the north of the Mohn Ridge, salinities are again overestimated. Layer 1 is the worst layer with maximum deviation of 0.4. Modelled salinities in the Greenland and Boreas Basin are too low, with the northernmost points in each basin as the worst. Layer 1 has the maximum underestimation of -0.5, while the average differences get smaller for each layer as one goes deeper.

The average temperature differences (model - Argo) are shown in Figure 5.12. The areas with over- and underestimations are not as distinct as for the salinity, but some features are still obvious. Starting with layer 4, which again has the best agreement between the model and the Argo data, we now discover some overestimation of temperatures in the Greenland Sea and some underestimations in the Lofoten Basin (Figure 5.12d). Deviations are not more than $\pm 0.5\,^{\circ}\mathrm{C}$. For the three upper layers there are in general too high model temperatures in the Norwegian Basin and the Greenland Sea while they are too low in the Lofoten Basin and in the two upper layers of the Boreas Basin. Points with over- and underestimation of temperature are more mixed compared to the salinity figure, especially in layer 1 (Figure 5.12a).

The temperature underestimations in the Lofoten Basin are almost similar in the two upper layers, with the largest differences of about $-1.5\,^{\circ}\mathrm{C}$ to the east. In layer 3 there are still some underestimation to the east, but the differences are less. In the middle of the basin even some small overestimations occur, with values of maximum $0.5\,^{\circ}\mathrm{C}$. In the deepest layer there are again mainly too low temperatures, but now the maximum underestimations are situated in the middle of the basin instead of to the east.

The water in layer 2 and 3 in the southern part of the Norwegian Basin is $3\,^{\circ}\mathrm{C}$ (or maybe more) too warm. The same is for layer 1, except that the temperatures are somewhat too cold in the southeastern part. To the north in the Norwegian Basin temperatures are about $1\,^{\circ}\mathrm{C}$ too high in the two upper layers, while both over- and underestimated temperatures occur next to each other in the third layer. Except from the Boreas Basin, the whole Greenland Sea has temperature overestimations of $3\,^{\circ}\mathrm{C}$

in layer 2 and 3. The same occur in the uppermost layer, except in the middle of the Greenland Basin where the differences are much less. In the Boreas Basin temperatures are most underestimated in layer 1, with a maximum of $-3\,^{\circ}\mathrm{C}$. Underestimations occur also in layer 2, but the differences are less. Layer 3 then has overestimations of about $1\,^{\circ}\mathrm{C}$ in the Boreas Basin.

Almost no differences were found while studying the maps where data from different months were extracted (not shown). The only exception was that from July to September there were no large temperature overestimations south in the Norwegian Basin in the uppermost layer. It never exceeded $1\,^{\circ}\mathrm{C}$ difference these months, but reached 2 and $3\,^{\circ}\mathrm{C}$ of overestimation during the period of February to June. Otherwise the figures from the three different periods showed that the tendencies were the same throughout the year.

All in all it seems like the warm and saline modelled Atlantic water is dispersed too much into the Norwegian Basin. That might be the reason for the underestimations in both temperature and salinity close to the coast of northern Norway, the model Atlantic Water never reaches this far north. The model is doing best in the deepest layer where the watermasses are most stable and hence easiest to model correctly.

To do some further investigation on the differences between Topaz and Argo, some representative profiles will be examined.

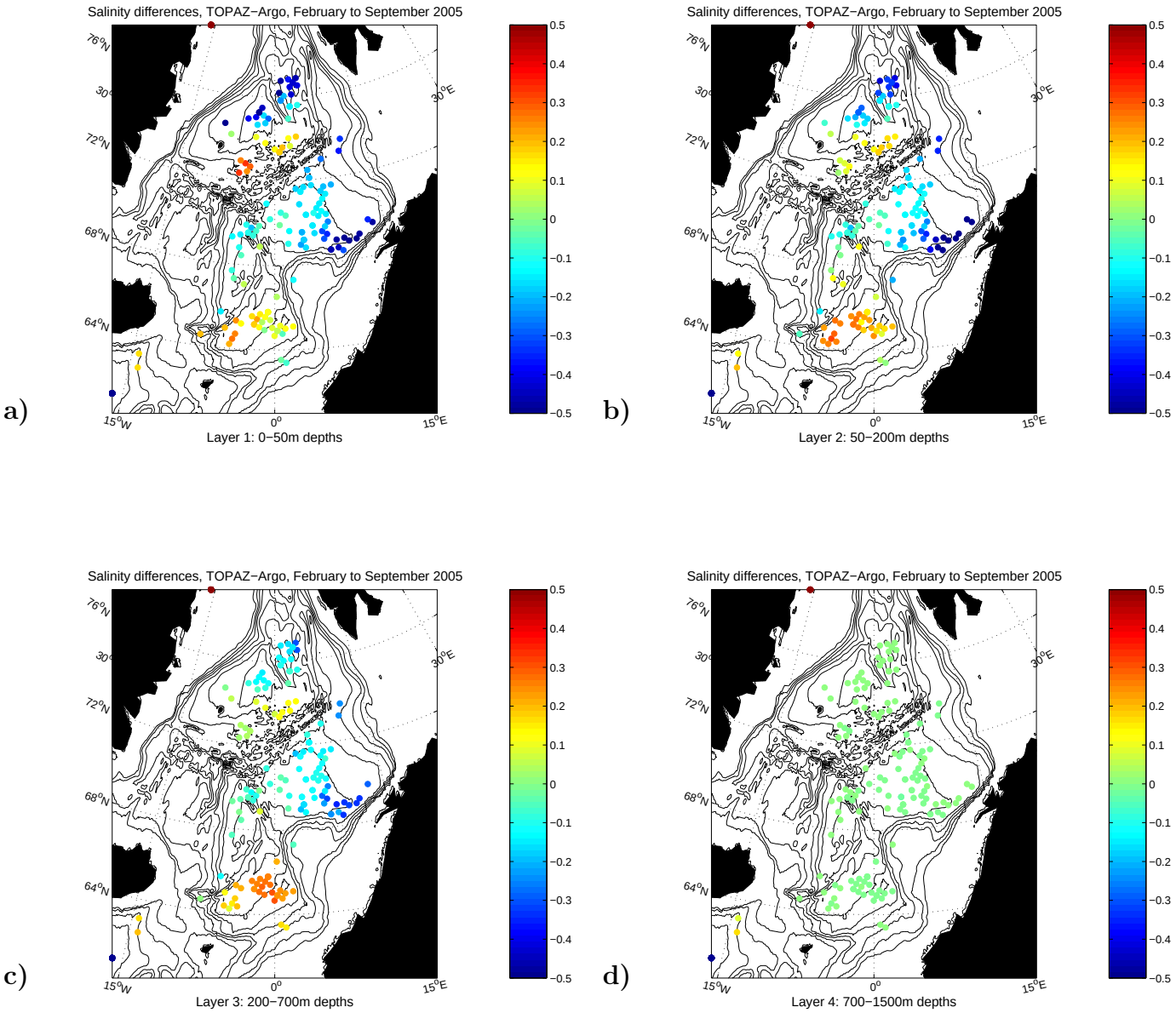

a) b) c) d)

Figure 5.11: ***Salinity differences, TOPAZ-Argo, February to September 2005 a) layer1: 0-50m b) layer2: 50-200m c) layer3: 200-700m d) layer4: 700-1500m***

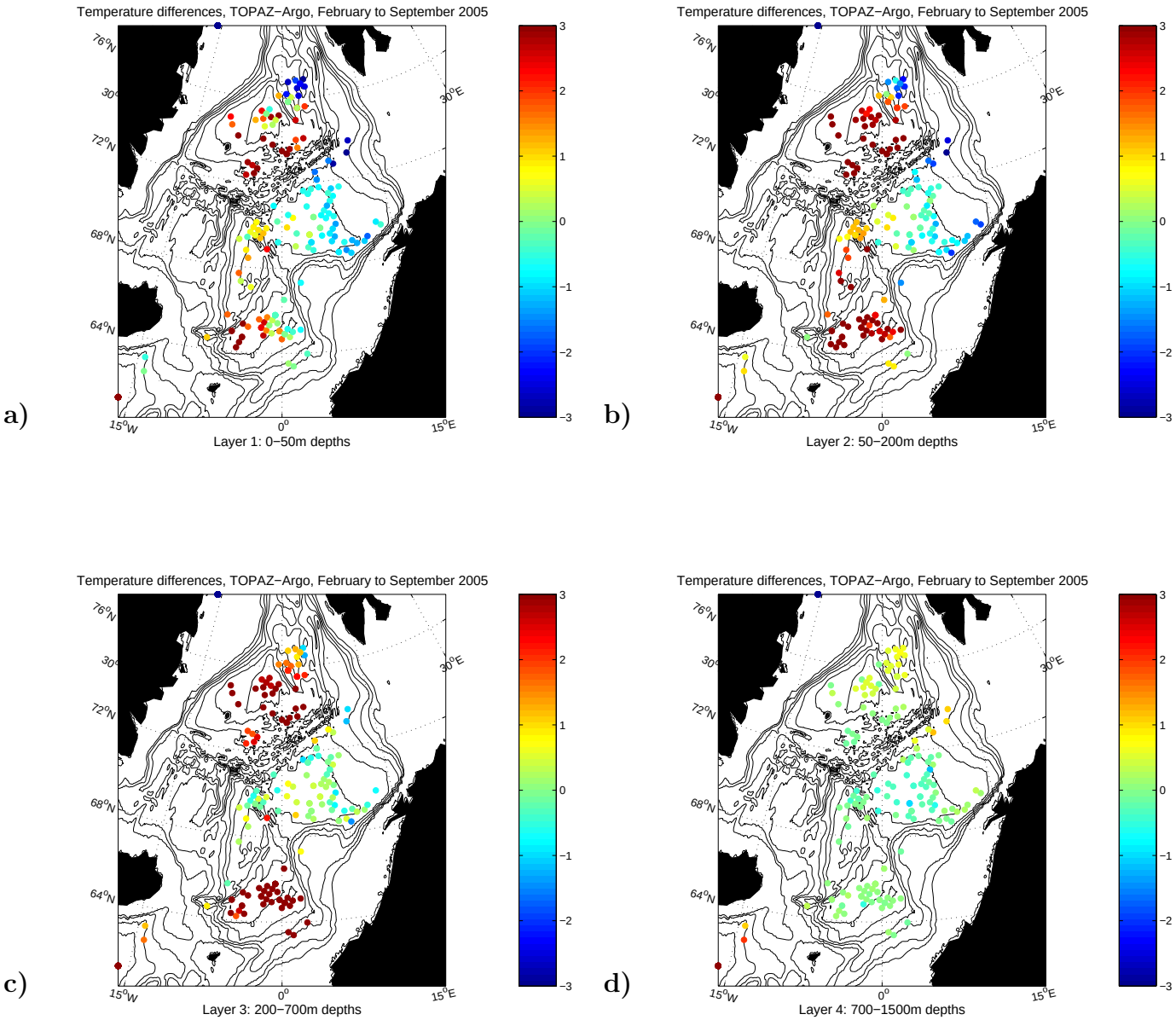

a) b) c) d)

Figure 5.12: ***Temperature differencese, TOPAZ-Argo, February to September -05 a) layer1: 0-50m b) layer2: 50-200m c) layer3: 200-700m d) layer4: 700-1500m.***

5.3.1 Comparison of single Argo and TOPAZ profiles

Several profiles from Argo and TOPAZ have been compared. Only a small selection will be presented here. Temperature profiles have been plotted against each other in the same grid, and the same is done for the salinity. Additionally each figure has a small map with a cross indicating where the profile was taken. Recall that we assume that the Argo data are the correct values for this purpose.

Norwegian Basin
Starting with the Norwegian Basin, Figure 5.13 shows profiles from 4 different locations. The profile in Figure 5.13a is typical for the southeastern part of this basin. It is taken the 4th of September 2005. The temperature profiles of Argo and the model have different shapes, and the thermocline of the modelled profile is approximately 400m too deep. This leads to an overestimation of the model temperature between 100 and 900m depths. Maximum deviation is 6 °C. Below 900m the modelled temperatures are good. In the surface layer the model temperature is slightly colder than what is measured by the Argo float. For the salinity profiles, Argo measures a maximum peak of 35.15 at 75 m depths, which the model does not maintain. Some of the Argo profiles in this area do not have this maximum salinity peak, it might be seasonally dependent. The model halocline is too deep, it is not that sharp and it has a convex curvature opposite to the concave Argo profile, just like the thermocline. This leads to a gap between the profiles between 0 and 700m depths, where model salinities are up to 0.25 too high. Below 700m depths the salinity profiles are in accordance with each other.

Figure 5.13b shows profiles from the southwestern part of the Norwegian Basin, taken the 27th of March 2005. Both the model temperature and salinity profile have almost similar characteristics as in Figure 5.13a. The Argo profiles have however more similar pattern as the model profiles here, but the size of the model gradients are larger than the Argo gradients for both temperature and salinity. Additional of too warm and saline model water at the surface, both the model thermocline and the model halocline are situated about 100m too deep compared to Argo. This leads to an overestimation of 4-5 °C of model temperatures between the surface and 400m depths, and some smaller overestimations down to 600m depths. Below this the agreement between the two temperature profiles is quite good. The salinity is about 0.25 too high from the surface and down to 300m depths, and from 300m to 500m depths the overestimations get smaller. Below 500m depths the salinity profiles are approximately similar. The large gap between the profiles in the upper layers indicate that the model overestimates the warm and saline Atlantic Water in the southern part of the Norwegian Basin.

The profiles in Figure 5.13c are taken the 24th of June 2005 in the mid west of the

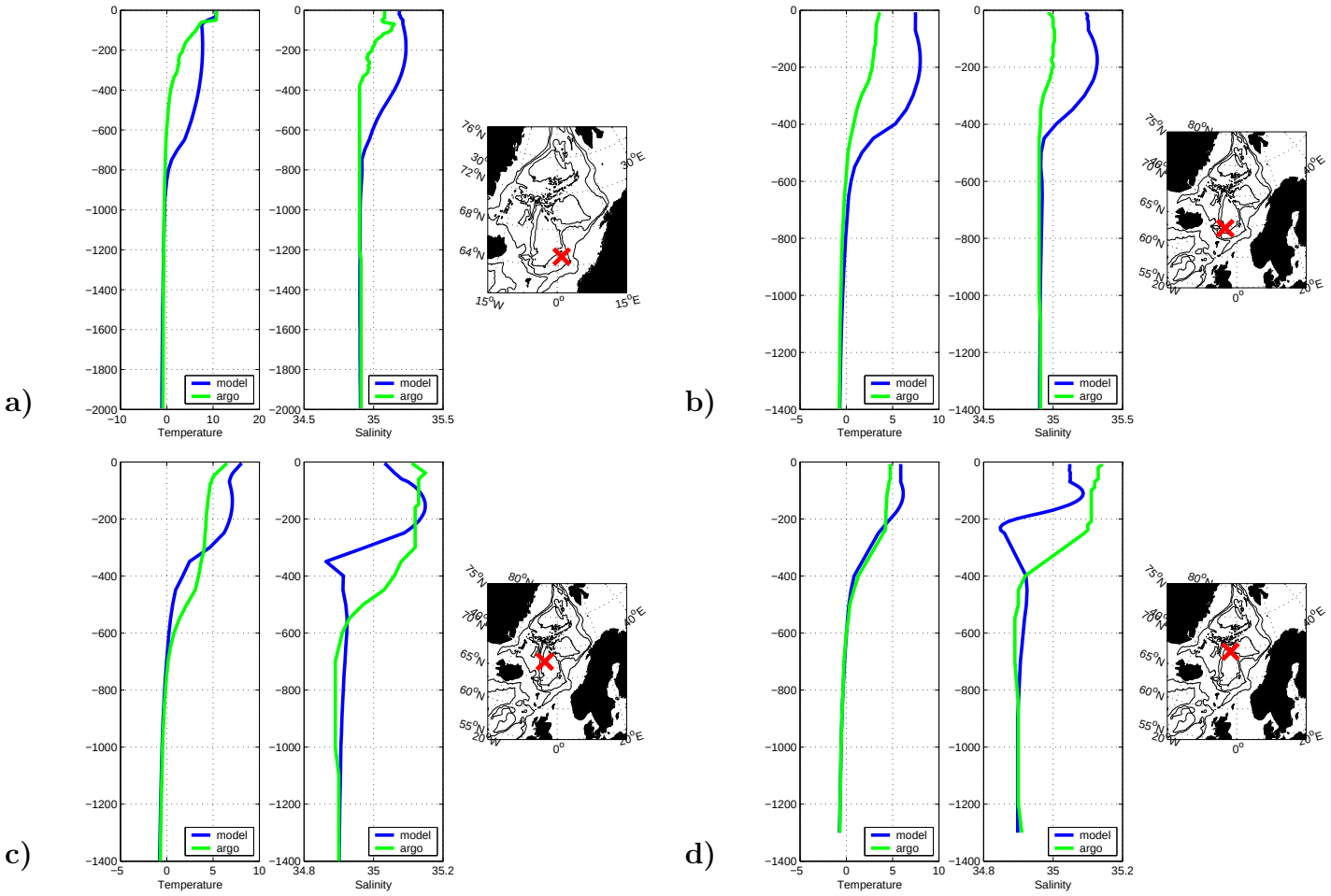

Figure 5.13: ***Argo (green) and model (blue) temperature and salinity profiles, respectively, in the Norwegian Basin.***

Norwegian Basin. The temperature profiles have to some extent similar patterns, but the modelled thermocline is too large and located about 100m too high in the water column. This results in model temperatures that are 2-3 °C too warm from 0-300m depths and about 1-2 °C too cold from 300-600m depths. Below this depth there are no differences between the profiles. The similarities among the salinity profiles are not that pronounced. In the upper layer, from 0-150m depths, the Argo profile is more vertical while the model profile is gradually decreasing with depth. Both profiles have a gradient ranging from about 35.1 to 34.9, but the model gradient is somewhat sharper and located 100-200m above the Argo gradient. This leads to an underestimation in the layer from 0-100m depths, with salinities around 0.5 too fresh. A small overestimation takes place between 100 and 200m depts, until salinities again are too fresh, around 0.15, down to 600m depths. Below this depth the salinities are nearly the same, although a bit overestimated down to 1100m depths. The salinity minimum obtained by Argo at these depths is the NSAIW.

The last profiles that will be shown from the Norwegian Basin are taken to the north at the 15th of February 2005, see Figure 5.13d. For the temperature profiles the agreement is quite good below 250m depths. The only failing is that the thermoclines ranging from 4 °C to 0.5 °C are situated 25m apart, with the model thermocline too high. This leads to 0.5 °C underestimated model temperatures between 250 and 500m depths. The modelled thermocline is larger than the Argo gradient and extends to 6 °C, which leads to overestimated model temperatures of 1-1.5 °C in the layer from 0-200m depths. The Argo salinity profile is like the Argo temperature profile nearly vertical down to 200m depths. In addition of 0.1 too fresh salinities in the surface layer, the model salinity profile has a rather sharp gradient between 100 and 200m depths. A similar gradient appears in the Argo profile, only 150-200m deeper. The result is underestimations of model salinities down to 400m depths, with maximum difference of 0.25. In the intermediate layer between 400 and 800m depths, the model salinities are about 0.02 too saline. Again Argo measures the salinity minimum of the NSAIW, while TOPAZ does not manage to model it. At greater depths the agreement is good.

Lofoten Basin

Profiles from three different locations within the Lofoten Basin are shown in Figure 5.14. The first (Figure 5.14a) is from the eastern part, taken the 10th of June 2005. Both the Argo and the model profiles are quite typical for this area. Looking at the temperature profiles, they have the same main features, but from the surface and down to 200m depths the model temperatures are underestimated by about 1 °C. The model thermocline is located about 100m too high, so that model temperatures between 400 and 1000m depths are 1-1.5 °C too cold. Below 1000m depths the agreement between the temperature profiles is quite good. For the salinity profiles there is a difference between Argo and the model all the way from the surface and down to 800m depths. The model salinities are mainly 0.25 too low, due to missing Atlantic Water. Below this the salinity profiles stick together.

Figure 5.14b shows profiles from the northern part of the Lofoten Basin, taken the 24th of February 2005. Some of the same features that were seen at the eastern part (Figure 5.14a) can also be seen here. The Argo temperature profile is very similar to the previous one, except in the upper layer where it is nearly vertical at 5 °C from 0-500m depths. Recall that this profile is taken in February, when the mixing layer is deeper due to seasonal phenomenon. The agreement between Argo and the model is however not that good. The model thermocline is not as step as Argo's, and it begins at 200m depths instead of 500m depths. This gives too low model temperatures down to 800m depths. Like in the eastern part, the two salinity profiles give a difference between Argo and the model from the surface and down to 800m depths. The model does

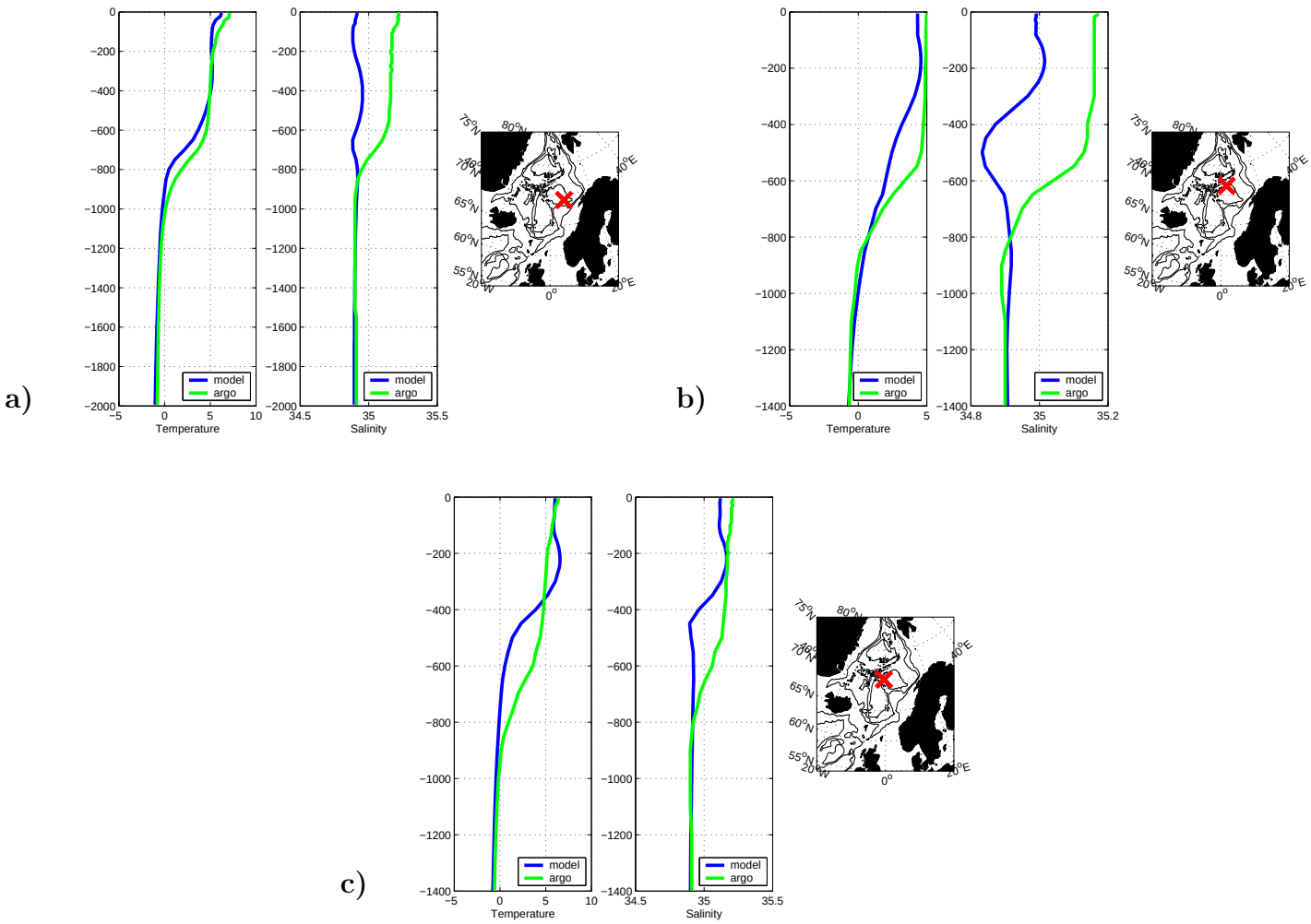

Figure 5.14: ***Argo (green) and model (blue) temperature and salinity profiles, respectively, in the Lofoten Basin.***

not maintain the real amount of Atlantic Water in the northern and eastern Lofoten Basin. Identifying the two haloclines, the model halocline is too short and located about 300m too high in the water column. From the surface to 200m depths the model salinity is therefore 0.15 too low, while the difference is up to 0.25 between 200-800m depths. Below 800m depths the agreement is fairly good for both the temperature and salinity profiles.

The last profiles from the Lofoten Basin are shown in Figure 5.14c. They are taken at the western part at the 4th of June 2005. The Argo profiles for both temperature and salinity are here quite similar as the previous profiles from the Lofoten Basin. From 0-50m depths the model temperatures are a bit underestimated while they are overestimated by 1-1.5 °C between 100-400m depths. The model thermocline is located about 200m above the Argo thermocline and hence the temperatures between

400-900m depths are underestimated by up to 3 °C. Below this both profiles show approximately the same values. Looking at the salinity profiles, the model layer between 0-200m depths is too fresh, about 0.1. Between 150-350m depths the model indicates a layer with maximum temperature and salinity that should not be present. At 200m depths both salinity profiles have the same values, but then salinities are underestimated down to 800m depths. This is because the model halocline is too steep, and like the model thermocline it is situated too high in the water column. Below 800m depths the agreement is quite good, except that the model does not make the salinity minimum between 900 and 1100m depths, indicating the NSAIW.

Greenland Sea

Profiles from the Greenland Sea are shown in Figure 5.15. The profiles from the Greenland Basin are taken the 16th of June 2005 (Figure 5.15a). The temperature profiles show that the model temperature is 1.5 °C too cold at the surface. Both profiles have steep thermoclines between the surface and 100m depths, but the model thermocline has a shorter range. From 200m to 2000m depths the Argo profile is approximately vertical at −1 °C, while the model profile is nearly vertical at about 2.5 °C between 100-600m depths. Then model temperatures down to 2000m depths are gradually decreasing. This gives overestimated model temperatures of about 3 °C between 100-600m depths and some smaller overestimations down to 1700m depths where the two profiles show the same temperatures again. The model salinities in the Greenland Basin are underestimated down to 600m depths. The difference is 0.3 at the surface. Between 100 and 600m depths the Argo profile is nearly vertical at 34.9 while the model profile has a salinity gradient ranging from 34.7 to 34.9. Between 600 and 2000m depths the agreement is quite good.

Figure 5.15b shows profiles from the Boreas Basin, taken the 24th of August 2005. The model temperature profile is similar to the one from the Greenland Basin. It is approximately vertical between 100 and 600m depths. Argo measures no traces of these homogenous temperatures. The Argo temperature profile from the Boreas Basin shows decreasing temperatures down to 400m depths. This gives underestimated model temperatures between 0-200m depths and overestimations between 200 and 2000m depths. The differences get smaller and smaller with depth. The model salinity profile has the same shape as the Greenland Basin profile between 0 and 600m depths, just a bit saltier. While the model salinities in this upper layer are increasing, the Argo profile shows decreasing salinity from 0 to 600m depths. This gives underestimated salinities, with the largest difference of 0.25 at the surface. Below 600m depths both the Argo and the model salinity profiles are quite similar to the profiles from the Greenland Basin, and both show similar values.

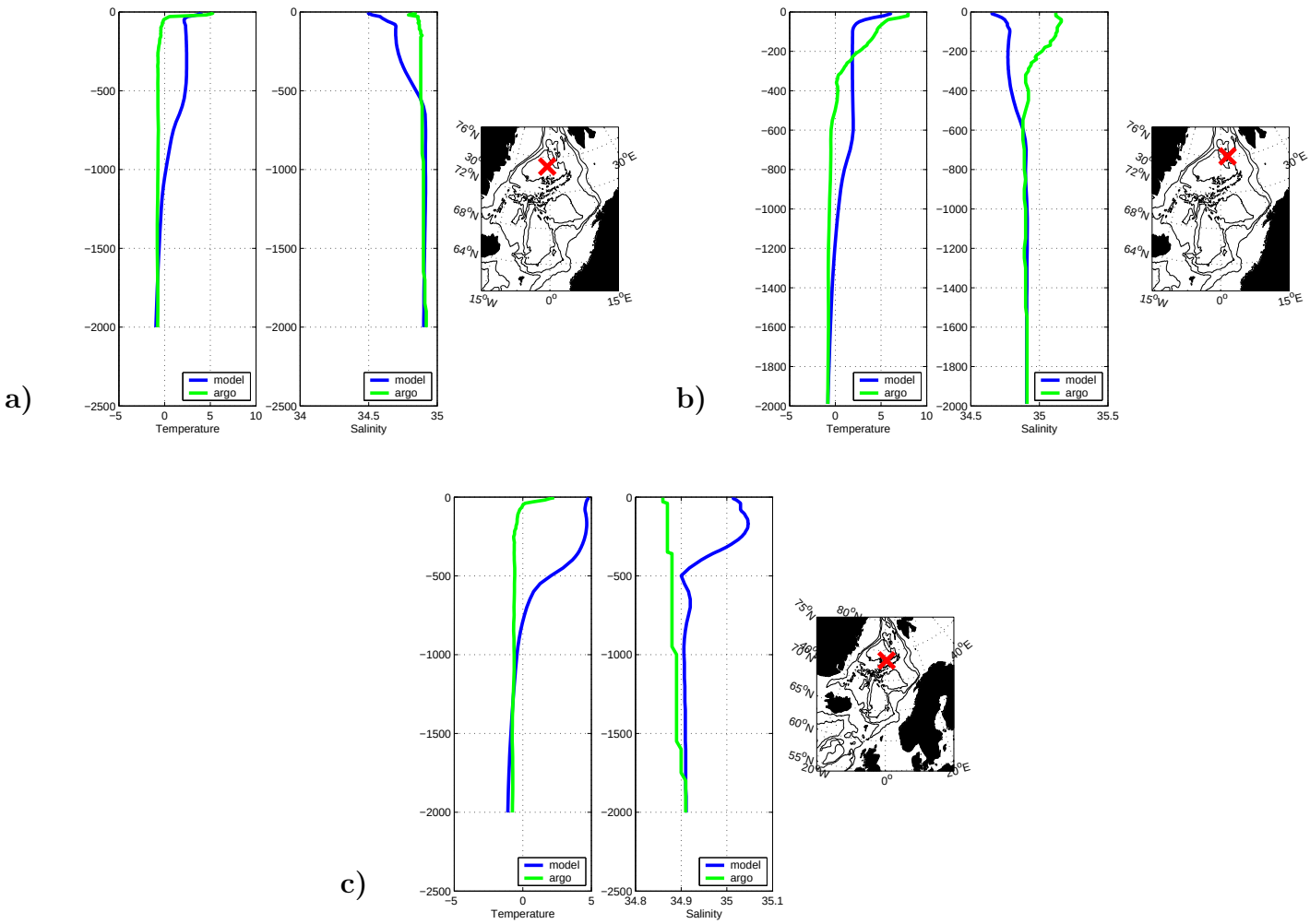

Figure 5.15: ***Argo (green) and model (blue) temperature and salinity profiles, respectively, in the Greenland Sea.***

The profiles in Figure 5.15c are taken south in the Greenland Sea, just north of the Mohn Ridge, at 15th of June 2005. The model thermocline is about 500m too deep. Additionally the model temperature is 2.5 °C too warm at the surface. Model temperatures are then overestimated by 4-5 °C down to 500m depths. The overestimations get smaller down to 1300m depths and below this the model temperatures are slightly underestimated. The model salinity profile has a gradient between 200-500m depths while the Argo profile has not. This leads to model salinities overestimated by 0.15 between 0-400m depths, contrary to the Greenland and Boreas Basin where model salinities were underestimated. Between 500 and 1800m depths the model salinity is slightly overestimated.

The study of single profiles within the Nordic Seas strengthens the assumptions that TOPAZ disperse too much of the Atlantic Water erroneously in the southern parts of

the Norwegian Basin. The model water in the upper layers is too warm and saline in this area. Consequently the upper layers in the eastern Lofoten Basin get too cold and fresh as too little of the model Atlantic Water reaches this far north. In the Greenland Sea there are areas with too warm and fresh model water in the upper layers, which is considered to be due to exaggerated mixing in TOPAZ. TOPAZ neither resolves the salinity minimum in the intermediate layer of NSAIW, as measured by Argo in the Norwegian Sea. It seems like the model have to coarse resolution to be able to permit a realistic circulation and to resolve the correct locations of the different watermasses.

Chapter 6

Summary and conclusions

This thesis provides an examination of the Argo profiling floats in the Nordic Seas. Per January 2006 there are more than 2200 Argo floats globally distributed, of which 28 are drifting in the Nordic Seas. For the first time we now have the opportunity to continuously monitor the ocean in near real-time. The Argo floats provide the main source of subsurface temperature and salinity measurements from the deep oceans. Additionally the drift of the Argo floats traces the currents at the parking depths. As the data are available in near real-time, which means within 24 hours, the possibilities for operational oceanography are great. Forecasting and observations on smaller scales like days or weeks will be improved as the number of floats increase and the data access are getting much better. At present, the 28 Argo floats that so far cover the whole Nordic Seas won't provide data with a spatial resolution that is good enough on such small time scales. On larger time scale it is envisioned that the resulting profiles will be used to initialize seasonal and decadal forecast models, calibrate/validate satellite altimetric data and assimilate data in the interior of the oceans. Impact of the assimilation of Argo data has already been found to be of great importance (Benkiran & Guinehut 2006). Argo will increase our understanding of the ocean and contribute to detect and attribute climate change effects on it.

The second source of data considered in this thesis is archived data from the TOPAZ model. It is an operational system for the whole Atlantic and Arctic Ocean, based on the hybrid coordinate ocean model HYCOM. Only results from the Nordic Seas are treated here.

Ocean Weather Station M (Mike) provides the longest time series of in situ measurements within the Nordic Seas. This data set has barely been used in this thesis, but a small comparison against the Argo data has been done.

The study of the Argo temperature and salinity profiles gave indications of the typical

conditions within the different basins and seas in the Nordic Seas. In the Norwegian and Lofoten Basin the conditions are quite similar in the surface layer, with temperatures ranging between 4-14 °C and salinities ranging between 34.7 and 35.3. A pronounced seasonal signal is seen. The bottom of the inflowing Atlantic water was found at 400-500m depths in the Norwegian Basin (NB) and at 600-800m depths in the Lofoten Basin (LB). The Norwegian Sea Arctic Intermediate Water, characterized by its salinity minimum (< 34.9), was identified at 500-950m depths in the NB while it was not that pronounced and located somewhat deeper in the LB. Below 1000m depths the Norwegian Sea Deep Water was found in both basins. For both the Greenland (GS) and Iceland Seas (IS) the surface waters are colder and fresher than in the Norwegian Sea. The GS has temperatures between -1 °C and 7 °C and salinities between 34.4 and 35.1. For the IS the surface temperatures range from 1-3 °C while the salinities are between 34.6 and 34.9 (note that measurements are from October-January only). Below 200m depths the watermasses are more homogenous.

Comparison of one single temperature and salinity profile was done between Argo and Mike. The measurements in deeper waters, below 800m depths, were in accordance with each other, indicating realistic values. The Mike profile was however warmer and saltier than the Argo profile in the upper part of the water column. The reason is considered to be that Mike is lying more into the North Atlantic Drift than the Argo float. It points out that frontal areas have large horizontal gradients demanding fine resolution models if the areas shall be well simulated.

The examination of the Argo trajectories and the estimated current velocities in the Nordic Seas showed that the deep-water currents in general are cyclonic within the basins. The depths that are considered are mainly 1500m in the Norwegian Sea and 1000m in the Greenland and Iceland Seas. The LB has the largest velocities with a mean of 6.3 cm/s, and also the largest seasonal variations. Mean velocity is 3.4 cm/s in the NB, 3.3 cm/s in the GS and 2.4 cm/s in the IS. The deep-water currents in the NB, LB and GS are strongest during the spring, but with maximum velocities earlier in the LB than in the NB and GS.

These findings coincide well with what was found by Mork & Skagseth (2005). They combined altimeter and hydrographic data to study the annual sea surface height (SSH) variability in the Nordic Seas. They also used this to calculate the seasonal anomalous bottom currents, relatively to the annual mean (see their figure 7). They found that the annual variations of the currents in the interior basins are aligned in the direction of the isobaths, with strongest cyclonic circulation during spring and weakest during autumn. By integrating the wind stress curl over an area within a closed bottom contour and comparing to the changes in the circulation, they found that the seasonal

strength of the bottom circulation is influenced by the seasonal wind forcing, at least in the Norwegian Sea. They also found that the seasonal SSH variation were larger in the LB than in the NB. For the IMR Argo data, Mork and Søiland (pers. com.) found that the wind stress curl is in phase with the change of speed in the LB. Hence it is likely that the seasonal velocity variations of deep waters in the Nordic Seas to a certain extent are wind forced.

Some of the Argo trajectories show a striking topographic steering of the deep-water currents. Of all the velocity estimates in the Nordic Seas, 35% deviate less than 30 ° from the calculated ideal topographic steering, but it is found that areas with larger bathymetry gradients are likely to have stronger topographic steering, while the drift above more flat areas tends to be more random. Some of the areas with largest mean bottom topography gradients have 80-100% velocity estimates that deviate less than 30 ° from the ideal topographic steering. The topographic steering is most prominent in the outer part of the NB and the LB. Almost no correlation were found between the bottom steepness and the speed.

This thesis also contains an intercomparison and brief validation of the TOPAZ system in the Nordic Seas. The results were however disappointing. Comparisons of the model against climatology and against the in situ Argo data showed that the inflowing warm Atlantic Water was too much dispersed into the middle of the Nordic Seas instead of following the Norwegian Atlantic Current northwards along the Norwegian coast. Down to 600-700m depths the model temperatures are too high in the southern NB, the southern GS and the IS, while it is too cold in the LB, the northern NB and the northern GS. The model mainly gives salinities that are too saline in the regions where temperatures are too high, and too fresh water in areas where temperatures are too low. An exception is the IS where the model salinities are too low. At greater depths where the physical properties of the water are more constant, the model versus climatology/Argo shows less difference.

The main reason for these results is considered to be the model resolution (>18km). Surface and deep-water currents were made from the TOPAZ model (not shown in this thesis), but with such erroneous results that they were not further examined. The Nordic Seas is a very dynamic area with a complex topography, which require high resolution to resolve the topographically steered circulation and permit the dominant physical processes that takes place. At present the inflow through the Faroe-Shetland channel is e.g. not realistic. The channel is very narrow and the model is not able to simulate realistic velocity vectors. In result the inflow of Atlantic Water is drifting in a somewhat wrong direction that disturbs the general circulation pattern for the whole Nordic Seas. However a new model run with double resolution is currently in

preparation (Bertino, MERSEA second year project report, in prep.) that yields more reliable model results.

Bibliography

Aagard, K. & Carmack, E. (1989), 'The role of sea ice and freshwater in the Arctic circulation.', *Journal of Gephysical Research* **94**, 14485–14498.

Benkiran, M. & Guinehut, S. (2006), 'Impact of the assimilation of Argo data in the Atlantic Mercator Operational Ocean Forecasting System.', *Coriolis News Letter* **2**.

Bentsen, M., Evensen, G., Drange, H. & Jenkins, A. D. (1999), 'Coordinate transformation on a sphere using conformal mapping', *Mon. Weather Rev.* **127**, 2733–2740.

Bertino, L. & Evensen, G. (2003), The DIADEM/TOPAZ monitoring and prediction system for the North Atlantic, *in* H. Dahlin, N. Flemming, K. Nittis & S. Petersson, eds, 'Building the European Capacity in Operational Oceanography, Proceedings of the Third International Conference on EuroGOOS, 3-6 December 2002, Athens, Greece', Vol. 69, Elsevier Oceanography Series, pp. 251–260.

Bertino, L., Lisæter, K. A., Sagen, H., Counillon, F., Winther, N., Stette, M., Natvik, L. J., Evensen, G., Morel, Y., Brankart, J. M., Birol, F., Brasseur, P., Verron, J., Schartau, M., Schroeter, J., Andreu Burillo, I., Dombrowsky, E., Larnicol, G., Schaeffer, P. & Weller, G. (2004), TOPAZ final report, Technical Report 251, Nansen Centre, Bergen, Norway.

Bleck, R. (2002), 'An oceanic general circulation model framed in hybrid isopycnic-Cartesian coordinates', *Ocean Modelling* **4**, 55–88.

Bleck, R. & Smith, L. (1990), 'A wind-driven isopycnic coordinate model of the North Atlantic and Equatorial Atlantic Ocean.1:Model development and supporting experiments', *Journal of Geophysical Research* **95**, 3273–3285.

Blindheim, J., Borovkov, V., Hansen, B., Malmberg, S.-A., Turell, W. & Østerhus, S. (2000), 'Upper layer cooling and freshening in the Norwegian Sea in relation to atmospheric forcing', *Deep Sea Research I* **47**, 655–680.

Blindheim, J. & Østerhus, S. (2005), The nordic seas, Main Oceanographic Features., *in* H. Drange, T. Dokken, T. Furevik, R. Gerdes & B. Wolfgang, eds, 'The Nordic

Seas: An Integrated Perspective', Geophysical Monograph Series 158, American Geophysical Union, pp. 11–37.

Brusdal, K., Brankart, J. M., Halberstadt, G., Evensen, G., Brasseur, P., van Leeuwen, P. J., Dombrowsky, E. & Verron, J. (2003), 'A demostration of ensemble-based assimilation methods with a layered OGCM from the perspective of operational ocean forecasting systems', *Journal of Marine Systems* **40-41**, 253–289.

Buch, E., Malmberg, S.-A. & Kristmannsson, S. (1996), 'Arctic Ocean deep water in the western Iceland Sea', *Journal of Geophysical Research* **101**, 11965–11973.

Carval, T., Keeley, B., Takatsuki, Y., Yoshida, T., Loch, S., Schmid, C., Goldsmith, R., Wong, A., McCreadie, R., Thresher, A. & Tran, A. (2006), Argo data management: User's manual, Version 2.1, Technical report, Ref ifremer: cor-do/dti-mut/02-084.

Drange, H., Dokkan, T., Furevik, T., Gerdes, R. & Berger, W. (2005b), *The Nordic Seas, An Integrated Perspective*, Geophysical Monograph Series 158, American Geophysical Union, Wahington DC. ISBN-0-87590-423-8.

Drange, H., Dokken, T., Furevik, T., R., G., Berger, W., Nesje, A., Orvik, K., Skagseth, Ø., Skjevlan, I. & Østerhus, S. (2005), The Nordic Seas: An Overview, *in* H. Drange, T. Dokken, T. Furevik, R. Gerdes & B. Wolfgang, eds, 'The Nordic Seas: An Integrated Perspective', Geophysical Monograph Series 158, American Geophysical Union, pp. 1–10.

Eldevik, T., Straneo, F., Sandø, A. B. & Furevik, T. (2005), Pathways and Export of Greenland Sea Water, *in* H. Drange, T. Dokken, T. Furevik, R. Gerdes & B. Wolfgang, eds, 'The Nordic Seas: An Integrated Perspective', Geophysical Monograph Series 158, American Geophysical Union, pp. 89–103.

Evensen, G. (1994), 'Sequential data assimilation with a nonlinear quasi-geostrophic model using Monte Carlo methods to forecast error statistics', *J. Geophys. Res.* **99**, 10,143–10,162.

Evensen, G. (2003), 'The ensemble Kalman filter: Theoretical formuliation and practical implementation', *Ocean Dynamics* **53**, 343–367.

Gammelsrød, T. & Holm, A. (1984), 'Variations of temperature and salinity at Station M (66N 27E) since 1948', *Rapp. P.-v. Run. Cons. int. Explor. Mer,* **185**, 188–200.

Gammelsrød, T., Østerhus, S. & Godøy, Ø. (1992), 'Decadal variations of ocean climate in the Norwegian Sea observed at Ocean Station "Mike" (66N 27E)', *ICES Mar. Sci. Symp.* **195**, 68–75.

Gill, A. E. (1982), *Atmosphere-Ocean Dynamics*, Academic Press, Inc. ISBN-0-12-283520-4.

Gould, J. (2002*a*), A beginners' guide to acceessing Argo data, Technical report, http://www.coriolis.eu.org//cdc/argo_rfc.htm.

Gould, J. (2002*b*), Data Management Handbook, Technical report, http://www.coriolis.eu.org//cdc/argo_rfc.htm.

Hansen, B. & Østerhus, S. (2000), 'North Atlantic-Nordic Seas exchanges', *Progress in Oceanography* **45**, 109–208.

Helland-Hansen, B. & Nansen, F. (1909), 'The Norwegian Sea, its physical oceanography. based upon the norwegian researches 1900-1904', *Report on Norwegian fishery and marine-investigations* **2**, 390.

Jakobsen, P., Ribergaard, M., Quadfasel, D., Schmith, T. & Hughes, C. (2003), 'Near surface circulation in the northern North Atlantic as inferred from Langrangian drifters: Variability from the mesoscale to interannual.', *Journal of Geophys. Res.* **108**, C8,DOI 10.1029/ 2002JC001554.

Mork, K. A. (2005), 'Monitoring the ocean climate with Argo floats', *Nordic Space Activities* **13**, 214–215.

Mork, K. A. & Skagseth, Ø. (2005), Annual sea surface height variability in the Nordic Seas, *in* H. Drange, T. Dokken, T. Furevik, R. Gerdes & B. Wolfgang, eds, 'The Nordic Seas: An Integrated Perspective', Geophysical Monograph Series 158, American Geophysical Union, pp. 51–64.

Mork, K. A. & Søiland, H. (2006), 'The deep circulation in the Norwegian Sea from subsurface drifters.', *Presentation at the Second Argo Science Workshop, Venezia* .

Nøst, O. A. & Isachsen, P. E. (2003), 'The large-scale time-mean ocean circulation in the Nordic Seas and Arctic Ocean estimated from simplified dynamics', *Journal of Marine Research* **61**, 175–210.

Orvik, K. & Niiler, P. (2002), 'Major pathways of Atlantic water in the northern North Atlantic and the Nordic Seas towards Arctic', *Geopphys. Res. Lett.* **29**, DOI 10.1029/2002GL015002.

Perry, R. K. (1986), Bathymetry, *in* B. G. Hurdle, ed., 'The Nordic Seas', New York: Springer, pp. 211–235.

Poulain, P.-M., Warn-Varnas, A. & Niiler, P. (1996), 'Near surface circulation of the Nordic Seas as measured by Langrangian drifters', *J. Geophys. Res.* **101**, C8, 18237–18258.

Rudels, B., Friedrich, H. & Quadfasel, D. (1999), 'The Arctic circumpolar boundary current', *Deep-Sea Research II* **46**, 1023–1062.

Svendsen, E., Sætre, R. & Mork, M. (1991), 'Features of the northern North Sea circulation', *Continental Shelf Research* **11**, 493–508.

Teague, W., Carron, M. & Hogan, P. (1990), 'A comparision between the Generalized Digital Environmental Model and Levitus climatologies', *JGR* **95**(C5), 7167–7183.

Vogt, P. R. (1986), Seafloor topography, sediments and paleoenvironments, *in* B. G. Hurdle, ed., 'The Nordic Seas', New York: Springer, pp. 337–410.